elucidated.[9–12] Excess energy intake, including high-fat diet (HFD), contributes to the development of metabolic syndrome. HFD also causes renal lipid accumulation and renal injury.[13] Therefore, elucidation of precise mechanisms that are responsible for renal lipid accumulation under an HFD could suggest the possible mechanisms underlying the development of renal injury in metabolic syndrome and thus enhance the design of novel therapeutic strategies against this renal injury.

Various intracellular molecules regulate local lipid metabolism in several tissues, such as skeletal muscle and liver.[14–17] Under an altered systemic glucose and lipid metabolism, the imbalance between lipogenesis and lipolysis in such tissues contributes to the local lipid accumulation and subsequent pathophysiologic changes.[16,18,19] However, in the kidney, the role of local lipid metabolism in lipid accumulation and subsequent renal injury in metabolic syndrome has not been fully determined.

The purpose of this study was to clarify further the role of renal lipid metabolism in the development of renal injury in metabolic syndrome. We first examined how HFD could affect renal lipid metabolism. We especially focused on the balance between lipogenesis and lipolysis in the kidney *per se*. Furthermore, we investigated how favorable systemic metabolic conditions under an HFD can affect renal lipid metabolism and renal injury by using heterozygous peroxisome proliferator–activated receptor-γ–deficient (*PPAR*-$\gamma^{+/-}$) mice, which were previously reported to be protected against HFD-induced obesity and insulin resistance.

RESULTS

Systemic Metabolic Abnormalities

The characteristics of the four groups at 16 wk of experimental period are presented in Table 1. *PPAR*-$\gamma^{+/+}$ mice on an HFD were significantly heavier than *PPAR*-$\gamma^{+/+}$ mice on a low-fat diet (LFD). These obese mice showed significantly high plasma triglycerides, cholesterol, TNF-α and monocyte chemoattractant protein-1 (MCP-1) levels, compared with their counterparts on an LFD. Plasma adiponectin levels in *PPAR*-$\gamma^{+/+}$ mice on an HFD were significantly lower than in *PPAR*-$\gamma^{+/+}$ mice on an LFD. Moreover, *PPAR*-$\gamma^{+/+}$ mice on an HFD showed hyperinsulinemia during 4 wk of HFD (Figure 1A) and hyperglycemia during 8 wk of HFD (Figure 1B). In contrast, *PPAR*-$\gamma^{+/-}$ mice were significantly protected against obesity, insulin resistance, and the altered adipokine secretions during the 16-wk HFD, although no differences in food intake were observed between *PPAR*-$\gamma^{+/+}$ and *PPAR*-$\gamma^{+/-}$ mice (Table 1, Figure 1, A and B). Glucose intolerance (determined by intraperitoneal glucose tolerance test) and insulin resistance (determined by intraperitoneal insulin tolerance test) at 16 wk of HFD in *PPAR*-$\gamma^{+/+}$ mice were attenuated in *PPAR*-$\gamma^{+/-}$ mice (Figure 1, C and D). *PPAR*-$\gamma^{+/+}$ mice showed features of metabolic syndrome from the early stage of HFD, whereas these alterations under an HFD were attenuated in insulin-sensitive *PPAR*-$\gamma^{+/-}$ mice, as previously reported.[20,21]

Renal Injuries

We confirmed the significant downregulation of mRNA expression of *PPAR*-γ in the kidneys of *PPAR*-$\gamma^{+/-}$ mice on both diets, compared with *PPAR*-$\gamma^{+/+}$ mice (Table 2). Under an HFD, *PPAR*-$\gamma^{+/+}$ mice exhibited a significant rise in urinary albumin excretion at 16 wk, although no significant differences were observed among the four groups at 4 and 8 wk (Figure 2). The increase in urinary albumin excretion at 16 wk was significantly inhibited in *PPAR*-$\gamma^{+/-}$ mice on an HFD (Figure 2). Examination of renal histopathologic changes with periodic acid-Schiff (PAS) in four groups revealed that HFD induced mesangial expansion in *PPAR*-$\gamma^{+/+}$ mice (Figure 3, B and M). The expression of fibronectin was significantly increased in both the glomeruli and interstitium of *PPAR*-$\gamma^{+/+}$ mice on an HFD (Figure 3, F and N, and J and O). In contrast, these HFD-induced glomerular and interstitial lesions were significantly attenuated in *PPAR*-$\gamma^{+/-}$ mice (Figure 3, D and M, H and N, and L and O). In both PPARγ$^{+/+}$ and PPARγ$^{+/-}$ on an LFD, glomerular and interstitial lesions were not observed (Figure 3, A, C, E, G, I, and K). Furthermore, under an HFD, the mRNA expression levels of fibronectin, type IV collagen, plasminogen activator-1, and MCP-1 were significantly increased in the renal cortex of *PPAR*-$\gamma^{+/+}$ mice, and these changes were significantly attenuated in *PPAR*-$\gamma^{+/-}$ mice (Table 2).

Table 1. Characteristics of the four groups of mice at the end of the 16-wk experimental period[a]

Characteristic	*PPAR*-$\gamma^{+/+}$ Mice		*PPAR*-$\gamma^{+/-}$ Mice	
	LFD	HFD	LFD	HFD
Body weight (g)	32.6 ± 2.9	45.2 ± 3.1[b,c]	31.2 ± 3.4	40.5 ± 2.8[b]
Food intake (g/d)	2.71 ± 0.17	2.57 ± 0.19	2.62 ± 0.22	2.58 ± 0.16
BP (mmHg)	91.0 ± 11.3	95.2 ± 8.7	92.1 ± 9.0	92.2 ± 14.7
Plasma triglyceride (mg/dl)	60.5 ± 14.5	156.0 ± 33.1[b]	86.2 ± 21	152.4 ± 21.3[b]
Plasma cholesterol (mg/dl)	122.3 ± 13.8	221.7 ± 18.9[b]	104.8 ± 10.9	201.3 ± 15.5[b]
Leptin (ng/ml)	4.56 ± 1.11	10.1 ± 3.11[b,c]	5.21 ± 1.22	16.5 ± 3.12[b]
Adiponectin (μg/ml)	8.21 ± 0.78	6.1 ± 0.31[b,c]	8.19 ± 0.21	7.89 ± 0.55
MCP-1 (ng/ml)	45.2 ± 11.1	154.0 ± 21.2[b,c]	47.0 ± 23.2	94.0 ± 13.9[b]
TNF-α (ng/ml)	9.50 ± 4.0	24.6 ± 4.6[b]	9.20 ± 3.1	19.9 ± 5.9[b]

[a]Data are means ± SEM; $n = 11$ in each group.
[b]$P < 0.05$ *versus* *PPAR*-$\gamma^{+/+}$ mice fed LFD.
[c]$P < 0.05$ *versus* *PPAR*-$\gamma^{+/-}$ mice fed HFD.

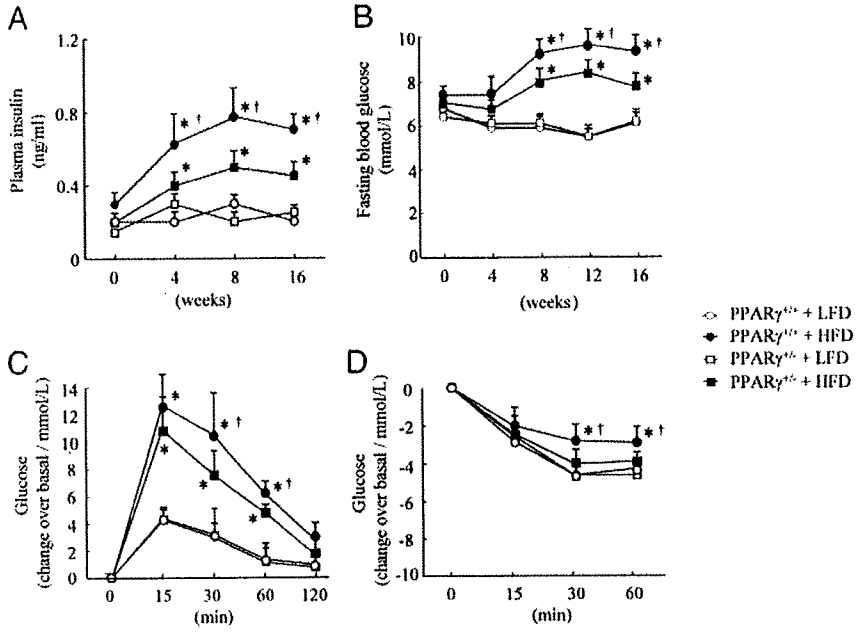

Figure 1. (A) Plasma insulin levels during 16-wk experimental period in each group of mice. Data are means ± SEM for five to 11 mice in each group. (B) Fasting blood glucose during 16-wk experimental period in each group of mice. Data are means ± SEM for 11 mice in each group. (C) Glucose tolerance test at the 16-wk experimental period in each group of mice. Data are means ± SEM for seven mice in each group. (D) Insulin tolerance test at the 16-wk experimental period in each group of mice. Data are means ± SEM for seven mice in each group. *$P < 0.05$ *versus PPAR-*$\gamma^{+/+}$ mice on an LFD; †$P < 0.05$ *versus PPAR-*$\gamma^{+/-}$ mice on an HFD.

Table 2. Levels of mRNA expression in the renal cortex at the end of 16-wk experimental period[a]

Parameter	*PPAR-*$\gamma^{+/+}$ Mice		*PPAR-*$\gamma^{+/-}$ Mice	
	LFD	HFD	LFD	HFD
PPAR-γ	0.95 ± 0.29	1.21 ± 0.23[b]	0.33 ± 0.13[c]	0.51 ± 0.12
Fibrosis and inflammation				
fibronectin	0.85 ± 0.16	1.31 ± 0.22[b,c]	0.70 ± 0.29	0.97 ± 0.03
type IV collagen	1.47 ± 0.18	2.10 ± 0.35[b,c]	1.43 ± 0.35	1.39 ± 0.21
PAI-1	0.81 ± 0.65	2.06 ± 0.37[b,c]	0.88 ± 1.22	0.98 ± 0.74
MCP-1	2.95 ± 1.22	5.73 ± 0.80[b,c]	2.89 ± 0.78	3.48 ± 0.33
Fatty acid synthesis				
SREBP-1c	1.66 ± 0.80	2.77 ± 0.62[b,c]	1.55 ± 0.71	1.82 ± 0.25
FAS	1.56 ± 0.56	5.22 ± 2.13[b,c]	1.34 ± 1.45	2.45 ± 0.88[c]
ACC	0.44 ± 0.19	3.70 ± 1.33[b,c]	0.54 ± 0.34	1.10 ± 0.34[c]
Fatty acid oxidation				
PPAR-α	1.81 ± 0.99	3.04 ± 0.45	1.93 ± 0.69	2.11 ± 0.40
CPT-1	2.82 ± 0.98	2.11 ± 0.87[b,c]	2.88 ± 0.34	5.12 ± 0.67[c]
ACO	0.84 ± 0.15	1.02 ± 0.15	1.03 ± 0.28	1.14 ± 0.25
MCAD	3.81 ± 0.79	3.01 ± 0.55	2.93 ± 1.49	4.11 ± 1.42

[a]Data are means ± SEM; $n = 11$ in each group. PAI-1, plasminogen activator-1.
[b]$P < 0.05$ *versus PPAR-*$\gamma^{+/-}$ mice fed HFD.
[c]$P < 0.05$ *versus PPAR-*$\gamma^{+/+}$ mice fed LFD.

Renal Lipid Accumulation

Increased renal triglyceride content was observed in *PPAR-*$\gamma^{+/+}$ mice at 8 and 16 wk of HFD, although no significant increase was observed at 4 wk of HFD (Figure 4A). Furthermore, HFD-induced increases in renal triglyceride content at 8 and 16 wk of HFD were significantly reduced in *PPAR-*$\gamma^{+/-}$ mice (Figure 4A). During the experimental period, no significant differences in renal cholesterol content were observed among the four groups (Figure 4B). Oil-Red O staining of kidney sections in the four groups revealed that HFD caused marked neutral lipid accumulations in both the glomerular and tubulointerstitial lesion (Figure 5, B and F). These accumulations were markedly decreased in *PPAR-*$\gamma^{+/-}$ mice (Figure 5, D and H). In both PPAR$\gamma^{+/+}$ and PPAR$\gamma^{+/-}$ on an

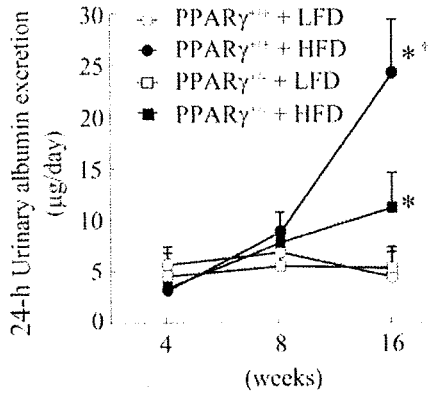

Figure 2. Twenty-four-hour urinary albumin excretion during the 16-wk experimental period in each group of mice. Data are means ± SEM for six to 11 mice in each group. $*P < 0.05$ *versus* *PPAR*-$\gamma^{+/+}$ mice on an LFD; $^{\dagger}P < 0.05$ *versus* *PPAR*-$\gamma^{+/-}$ mice on an HFD.

LFD, these renal neutral lipid accumulations were not observed (Figure 5, A, C, E, and G).

Renal Lipid Metabolism

Sterol regulatory element-binding protein-1c (SREBP-1c) is a transcriptional factor that regulates the transcriptional activity of the enzymes that are involved in lipogenesis, fatty acid synthase (FAS) and acetyl-CoA carboxylase (ACC).[17,22] In the kidneys from all four groups, we measured the mRNA expressions of SREBP-1c, FAS, and ACC at 4 and 16 wk. The mRNA expression levels of these molecules were increased in the kidneys of *PPAR*-$\gamma^{+/+}$ mice on an HFD at both time points (Tables 2 and 3). However, these changes were not observed in *PPAR*-$\gamma^{+/-}$ mice (Tables 2 and 3). Furthermore, under an HFD, ACC protein content was increased in the kidneys of *PPAR*-$\gamma^{+/+}$ mice at 16 wk but not in *PPAR*-$\gamma^{+/-}$ mice (Figure 6, A and B).

We next measured the mRNA expression levels of the molecules that are involved in lipolysis. At both 4 and 16 wk, we did not observe any differences in mRNA expression levels of PPAR-α, acyl-CoA oxidase, (ACO), and acyl-COA dehydrogenase (MCAD) in the kidneys among the four groups (Tables 2 and 3). However, at both 4 and 16 wk of HFD, a significant decrease in mRNA expression of carnitine palmitoyl transferase-1 (CPT-1) in the kidney of *PPAR*-$\gamma^{+/+}$ mice was observed, although this was not found in *PPAR*-$\gamma^{+/-}$ mice (Tables 2 and 3).

The 5′ AMP-activated protein kinase (AMPK) phosphorylates and inactivates ACC, resulting in a decrease in intracellular level of malonyl-CoA, thereby relieving inhibition of CPT-1 activity and accelerating lipolysis.[23] Phosphorylation of both AMPKα(Thr172) (Figure 6, A and C) and ACC(Ser79) (Figure 6, A and D) were significantly decreased in the kidneys of *PPAR*-$\gamma^{+/+}$ mice on an HFD at 16 wk. In contrast, these HFD-induced decreases in phosphorylation of AMPKα(Thr172) (Figure 6, A and C) and ACC(Ser79) (Figure 6, A and D) were not observed in the *PPAR*-$\gamma^{+/-}$ mice.

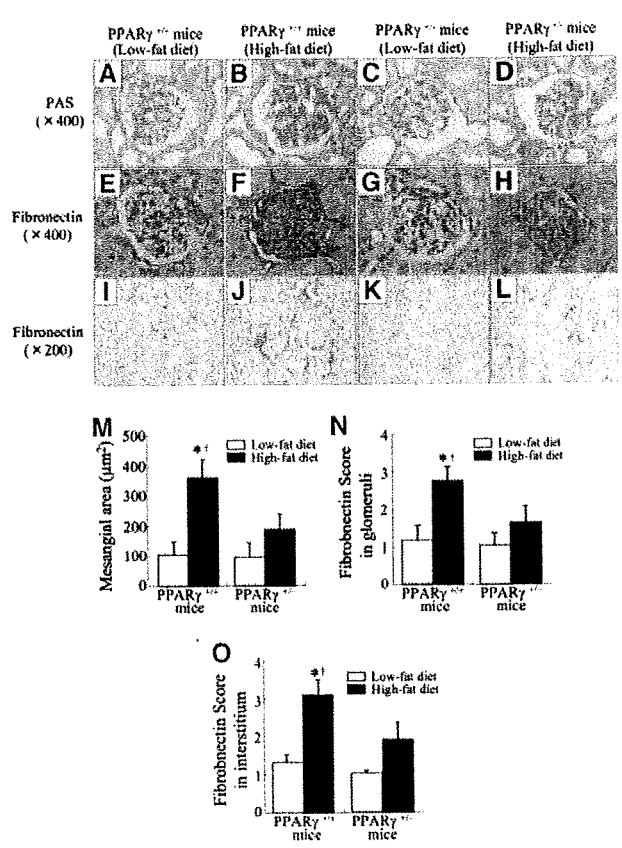

Figure 3. (A through D) Representative photomicrographs of PAS-stained kidney sections from mice in each group. (E through H) Representative photomicrographs of glomeruli of kidney sections immunostained for fibronectin. (I through L) Representative photomicrographs of interstitium of kidney sections immunostained for fibronectin. (M) Quantitative analysis of mesangial area from 20 glomeruli per mouse. Data are means ± SEM for 11 mice in each group. (N) Quantitative analysis of fibronectin score from 20 glomeruli per mouse. Data are means ± SEM for 11 mice in each group. (O) Quantitative analysis of fibronectin score from 20 random fields per mouse. Data are means ± SEM for 11 mice in each group. $*P < 0.05$ *versus* *PPAR*-$\gamma^{+/+}$ mice on an LFD; $^{\dagger}P < 0.05$ *versus* *PPAR*-$\gamma^{+/-}$ mice on an HFD. Magnifications: ×400 in A through H; ×200 in I through L.

DISCUSSION

Here, we show that HFD induces the alteration of renal lipid metabolism by an imbalance between lipogenesis and lipolysis in the kidney *per se*, as well as systemic metabolic abnormalities and subsequent renal lipid accumulation and renal injury. Furthermore, these renal involvements under an HFD are ameliorated in insulin-sensitive *PPAR*-$\gamma^{+/-}$ mice.

Recently, HFD was reported to induce renal injury, although the exact mechanisms have not been fully clarified.[13,24] Several reports have suggested that renal lipid accumulation, lipotoxicity, is associated with the development of such renal injury.[13] It is interesting that our results show that HFD induces systemic metabolic abnormalities such as insulin resis-

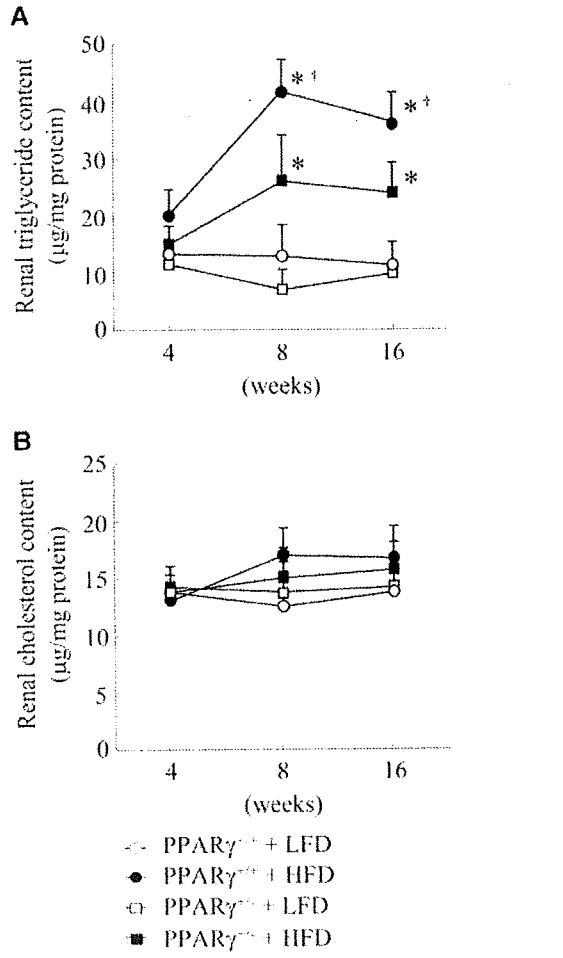

Figure 4. Triglyceride (A) and cholesterol (B) contents in the kidneys of mice in each group. Data are means ± SEM for five to 11 mice in each group. $^{*}P < 0.05$ *versus PPAR-*$\gamma^{+/+}$ mice on an LFD; $^{\dagger}P < 0.05$ *versus PPAR-*$\gamma^{+/-}$ mice on an HFD.

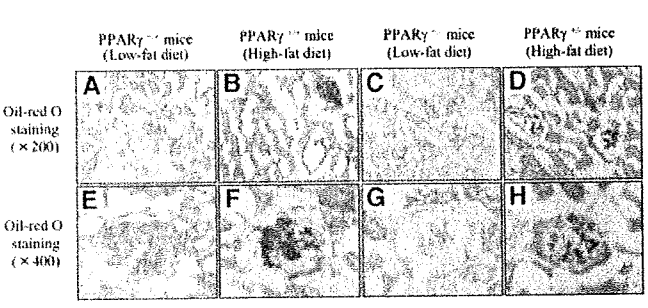

Figure 5. (A through H) Representative photomicrographs of Oil-Red O–stained kidney sections in each group of mice. Magnifications: ×200 in A through D; ×400 in E through H.

tance during 4 wk of HFD and subsequent renal lipid accumulation during 8 wk of HFD and finally renal injury at 16 wk of HFD. Furthermore, these HFD-induced renal involvements are ameliorated in insulin-sensitive *PPAR-*$\gamma^{+/-}$ mice. These results suggest that lipotoxicity in the kidney could be one of the important mechanisms for the development of renal injury associated with metabolic syndrome.

To date, the precise mechanisms for renal lipid accumulation have not been fully determined. However, there is growing evidence that the increased renal lipogenesis plays a role in the pathogenesis of renal injury.[11,13,25,26] Therefore, we investigated whether HFD increases renal mRNA expression levels of SREBP-1c, FAS, and ACC, which are involved in lipogenesis. Similar to previous reports,[11,13,25,26] mRNA expression levels of these molecules were increased in the kidneys of *PPAR-*$\gamma^{+/+}$ mice during 4 wk of HFD, whereas these were not observed in the kidneys of insulin-sensitive *PPAR-*$\gamma^{+/-}$ mice. Therefore, we can show that the increase in renal lipogenesis is observed from the early stage of HFD, before neutral lipid accumulation in the kidney. These observations provide further evidence that the accelerated renal lipogenesis contributes to the development of renal lipid accumulation under insulin resistance.

In addition to renal lipogenesis, we examined the effects of HFD on renal lipolysis to determine its role in the development of renal lipid accumulation. Our results showed that mRNA expression levels of CPT-1, which is one of the key enzymes involved in lipolysis, were significantly decreased during the 4 wk of HFD but not in *PPAR-*$\gamma^{+/-}$ mice. These results suggest that renal lipolysis decreases under insulin resistance, which may contribute to renal lipid accumulation. PPAR-α also regulates lipolysis in various tissues.[27] However, we failed to find significant differences of renal mRNA expression levels of PPAR-α among the four groups. Furthermore, we could not observe differences of renal mRNA expression of ACO and MCAD, which are transcriptional target molecules of PPAR-α. These results suggest that HFD might not affect mRNA expression of PPAR-α or activity of PPAR-α in this mouse model of metabolic syndrome.

In this study, we found decreased renal mRNA expression levels of CPT-1, although those of ACO, MCAD, and PPAR-α were not changed, in *PPAR-*$\gamma^{+/+}$ mice on an HFD. We therefore focused on the activity of the AMPK pathway to explore this discrepancy, because this pathway is a key regulator of intracellular lipid metabolism in other tissues[23] and because activated AMPK inactivates ACC, resulting in a decrease in malonyl-CoA, with subsequent release of inhibition of CPT-1 expression levels and acceleration of lipolysis.[23] Under an HFD, phosphorylation of AMPKα(Thr172) and ACC(Ser79) was significantly decreased in the kidneys of *PPAR-*$\gamma^{+/+}$ mice but not in the kidneys of *PPAR-*$\gamma^{+/-}$ mice. These results suggest that decreased AMPKα activity in the kidney under an HFD could increase the activity of ACC and intracellular malonyl-CoA content, resulting in the decreases in renal mRNA expression of CPT-1. These results could provide new evidence that a decrease in lipolysis *via* inhibiting the AMPK–CPT-1 pathway but not PPAR-α could contribute to renal lipid accumulation under an HFD. Furthermore, these results suggest that posttranslational activation of ACC by inhibiting AMPK activity under an HFD might contribute to the acceleration of renal lipogenesis, as well as increased renal expression of ACC.

Table 3. Levels of mRNA expression in the renal cortex at 4 wk[a]

Parameter	*PPAR-γ*$^{+/+}$ Mice		*PPAR-γ*$^{+/-}$ Mice	
	LFD	HFD	LFD	HFD
Fatty acid synthesis				
SREBP-1c	1.21 ± 0.10	2.93 ± 0.31[b,c]	1.29 ± 0.10	1.69 ± 0.16
FAS	1.54 ± 0.15	3.38 ± 0.67[b,c]	1.63 ± 0.17	1.72 ± 0.15
ACC	0.57 ± 0.07	1.06 ± 0.17[b,c]	0.59 ± 0.04	0.69 ± 0.13
Fatty acid oxidation				
PPAR-α	2.13 ± 0.61	3.13 ± 0.60	2.18 ± 0.24	2.78 ± 0.34
CPT-1	3.20 ± 0.29	2.03 ± 0.47[b,c]	3.04 ± 0.35	2.77 ± 0.20
ACO	0.91 ± 0.22	1.09 ± 0.22	1.02 ± 0.28	0.90 ± 0.13
MCAD	3.56 ± 1.89	3.89 ± 1.10	4.45 ± 2.14	3.95 ± 1.50

[a]Data are means ± SEM; $n = 5$ to 6 in each group.
[b]$P < 0.05$ *versus PPAR-γ*$^{+/+}$ mice fed LFD.
[c]$P < 0.05$ *versus PPAR-γ*$^{+/-}$ mice fed HFD.

In this study, we show that the improvements of systemic metabolic abnormalities result in the attenuation of HFD-induced renal lipid accumulation and renal injury with the improvement of renal lipid metabolism in *PPAR-γ*$^{+/-}$ mice. We previously reported that moderate reduction of PPAR-γ activity could decrease local lipid accumulation in the liver and skeletal muscle in *PPAR-γ*$^{+/-}$ mice.[20] These results raise the question of whether the reduction of PPAR-γ activity could directly affect the improvement of renal lipid metabolism in the kidneys of *PPAR-γ*$^{+/-}$ mice on an HFD. Liver-specific PPAR-γ disruption could attenuate steatohepatitis with the reduction of lipid accumulation in leptin-deficient mice.[28] Also, deletion of PPAR-γ in adipose tissues of mice protects against HFD-induced adipocyte hypertrophy, which inhibits obesity and insulin resistance.[29] These reports suggest that a reduction of PPAR-γ activity may inhibit various diseases that are associated with local lipid accumulation in various peripheral tissues, including kidney. However, our study does not provide enough evidence to clarify whether PPAR-γ deficiency in the kidney directly regulates renal lipid metabolism, as well as other peripheral tissues.[28,29] Further studies are required to determine the direct effects of PPAR-γ activity on renal lipid metabolism.

Several investigators have reported that PPAR-γ agonists can protect against the various types of renal injury through their anti-inflammatory and antifibrotic effects.[30–32] In contrast, our results showed that systemic reduction of PPAR-γ expression could improve HFD-induced renal injury. We therefore suggest that both PPAR-γ agonists and PPAR-γ insufficiency in the absence of ligands can protect against renal injury that is associated with glucose and lipid metabolism abnormalities, at least in part, through the attenuation of both systemic and renal lipid metabolism. Furthermore, several reports show that PPAR-γ recruits other transcriptional co-repressor complexes in the absence of ligand and that these co-repressors are capable of down-regulating PPAR-γ–mediated transcriptional activity.[33,34] This might be another mechanism through which both ligand binding to PPAR-γ and ligand-free PPAR-γ deficiency could promote renal protection.

Here, we present evidence that HFD causes renal lipid accumulation and renal injury with increased renal lipogenesis and decreased renal lipolysis, whereas these abnormalities are attenuated in insulin-sensitive *PPAR-γ*$^{+/-}$ mice. These results suggest that the improvement of an imbalance between renal lipogenesis and lipolysis results in a reduction of renal lipid accumulation and subsequent attenuation of renal injury under insulin resistance. Therefore, we propose that attenuation of renal lipid metabolism could serve as a new therapeutic strategy to prevent the development of CKD in metabolic syndrome.

CONCISE METHODS

Animal Models

PPAR-γ$^{+/-}$ mice were generated as described previously.[21] Six-week-old mice were housed in box cages, maintained on a 12-h light/12-h dark cycle, and fed an LFD (10% of kilocalories from fat) or HFD (45% of kilocalories from fat) obtained from Research Diets (New Brunswick, NJ) for 16 wk. At the end of 16-wk period, body weight, BP, and blood glucose were measured. BP of conscious mice was measured at a steady state with a programmable tail-cuff sphygmomanometer (BP98-A; Softron, Tokyo, Japan). Mice were placed in metabolic balance cages for 24-h urine collection to measure albumin concentration. Mice were anesthetized and perfused as described previously.[11] The right kidney was embedded in paraffin for PAS staining and immunohistochemistry or was frozen for Oil-Red O staining. Total RNA and protein were extracted from the remaining renal cortex of the left kidney. The Research Center for Animal Life Science of Shiga University of Medical Science approved all experiments.

Antibodies

Anti–phospho-acetyl CoA carboxylase(Ser79) was obtained from Upstate Cell Signaling (Lake Placid, NY). Anti–phospho-AMPKα(Thr172), anti-AMPKα(23A3), and anti-ACC were from Cell Signaling Technology (Beverly, MA).

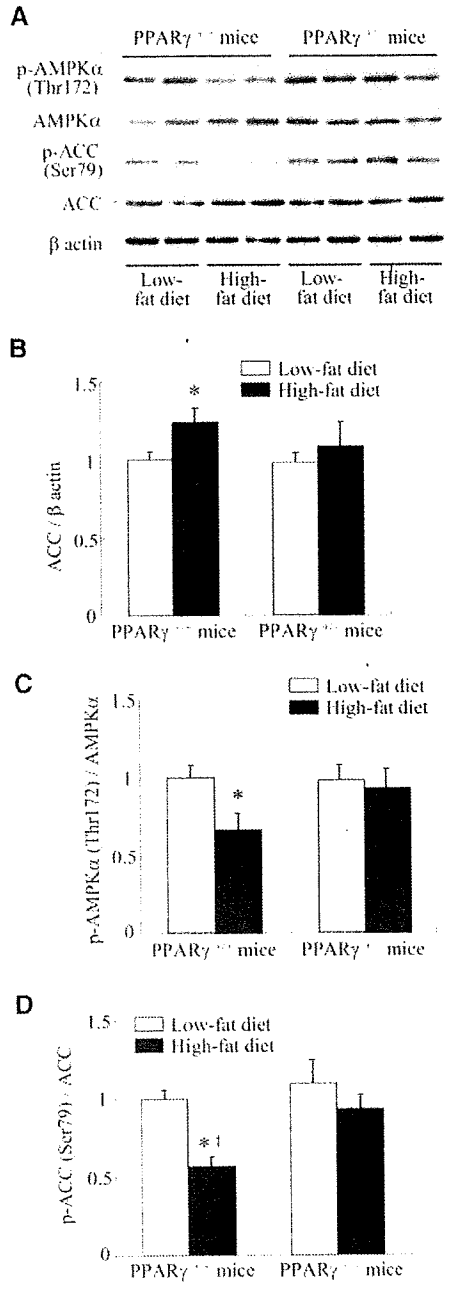

Figure 6. (A) Representative immunoblots of phospho-AMPKα(Thr172), AMPKα, phospho-ACC(Ser79), and ACC in the protein extractions from renal cortex of mice in each group. β-Actin was loaded as an internal control. (B) Quantitative analysis of ACC protein expression. (C) Quantitative analysis of phospho-AMPKα(Thr172). (D) Quantitative analysis of phospho-ACC(Ser79). Data are means ± SEM for five to eight mice in each group. $^{*}P < 0.05$ *versus PPAR-*$\gamma^{+/+}$ mice on an LFD; $^{\dagger}P < 0.05$ *versus PPAR-*$\gamma^{+/-}$ mice on an HFD.

Blood and Urine Analysis

Cholesterol or triglycerides were measured using the cholesterol CII kit or L type TG H kit (Wako Chemicals, Richmond, VA). Plasma insulin was determined using an ELISA (Exocell, Philadelphia, PA). Plasma leptin, MCP-1, and TNF-α were assayed with the immunoassay kit (R&D Systems, Minneapolis, MN). Plasma adiponectin was determined with a mouse-specific ELISA kit (Linco Research, St. Charles, MO). Urinary albumin excretion was measured with a mouse-specific sandwich ELISA system (Albuwell; Exocell) and was expressed as total amount excreted in 24 h.

Protein Extraction and Western Blot Analysis

The renal cortex was homogenized in an ice-cold lysis buffer containing 150 mmol/L NaCl, 50 mmol/L Tris-HCl (pH 8.0), 0.1% SDS, 1% Nonidet P-40, and protease inhibitor cocktail (Boehringer Mannheim, Lewes, UK). These samples were resolved by 10% SDS-PAGE and transferred to polyvinylidene fluoride membranes (Immobilon, Bedford, MA). The membranes were incubated with the appropriate antibodies, washed, and incubated with horseradish peroxidase–coupled secondary antibodies (Amersham, Buckinghamshire, UK). The blots were visualized by using an enhanced chemiluminescence detection system (Perkin Elmer Life Science, Boston, MA).

RNA Extraction and Quantitative Real-Time PCR

Total RNA was isolated from the renal cortex based on the TRIzol protocol (Invitrogen Life Technologies, Carlsbad, CA). cDNA was synthesized using reverse transcript reagents (Takara, Otsu, Japan). iQSYBR Green Supermix (Bio-Rad Laboratories, Hercules, CA) was used for real-time PCR (ABI Prism TM 7500 Sequence Detection System; Perkin-Elmer Applied Biosystems). The levels of mRNA expression of these molecules were quantified using standard curve method. Standard curves were constructed using serially diluted standard template. C_t value was used to compute the levels of mRNA expression from the standard curve. Analytical data were adjusted with the levels of mRNA expression of β-actin as an internal control. Primers used are described in Table 4.

Lipid Extraction and Analysis

Total lipid was extracted from the renal cortex by the method of Bligh and Dyer.[35] Triglyceride and cholesterol contents were determined as described previously.

Morphologic Analysis

Fixed kidneys were embedded in paraffin, sectioned (3-μm thick), and then stained with PAS reagent as described previously.[36] From each mouse, 20 glomeruli cut at their vascular poles were used for morphometric analysis. The extent of the mesangial matrix (defined as mesangial area) was determined by assessment of the PAS-positive and nucleus-free area in the mesangium using a computer-assisted color image analyzer (LUZEX F; Nikon, Tokyo, Japan). Immunohistochemical staining was performed with fibronectin-specific polyclonal anti-mouse antibody (A852/R5H; Biogenesis, Poole, UK). For evaluation of immunostaining for fibronectin, the percentages of area stained for fibronectin were graded as follows: 0, staining absent to 5%; 1, 5 to 25%; 2, 25 to 50%; 3, 50 to 75%; and 4, >75%.[36] An investigator who was masked to sample identity performed the image analysis. Frozen sections were used for Oil-Red O staining, as previously reported.[11]

Table 4. Primer sequences for real-time PCR

Primer	Forward	Reverse
β-actin	CGTGCGTGACATCAAAGAGAA	TGGATGCCACAGGATTCCAT
Fibronectin	GCAAGCCAGTTTCCATCAAT	CATTTTTGGGAGTGGTGGTCA
Type IV collagen	TACCTGCCACTACTTCGCTAAC	CGGATGGTGTGCTCTGGAAG
PAI-1	GGACACCCTCAGCATGTTCA	TCTGATGAGTTCAGCATCCAAGAT
MCP-1	GCCCCACTCACCTGCTGCTACT	CCTGCTGCTGGTGATCCTCTTGT
SREBP-1c	GGAACCATGGATTGCACATT	AGGAAGGCTTCCAGAGAGGA
FAS	CCTGGATAGCATTCCGAACCT	AGCACATCTCGAAGGCTACACA
ACC	CCCAGCAGAATAAAGCTACTTTGG	TCCTTTTGTGCAACTAGGAACGT
CPT-1	ACCACTGGCCGAATGTCAAG	AGCGAGTAGCGCATGGTCAT
PPARα	CTGCAGAGCAACCATCCAGAT	GCCGAAGGTCCACCATTTT
PPARγ	CACAATGCCATCAGGTTTGG	GCTGGTCGATATCACTGGAGATC
ACO	GGCCAACTATGGTGGACATCA	ACCAATCTGGCTGCTGCACGAA
MCAD	TAATCGGTGAAGGAGCAGGTTT	GGCATACTTCGTGGCTTCGT

Glucose Tolerance Test and Insulin Tolerance Test

For glucose tolerance tests, mice were fasted overnight for 14 h followed by intraperitoneal glucose injection (1 g/kg body wt). Blood glucose was measured using tail blood collected at 0, 15, 30, 60, and 120 min after the injection.[37] For insulin tolerance tests, mice were administered an injection of human regular insulin (Novolin R; Novo Nordisk, Clayton, NC) at 0.75 U/kg body wt intraperitoneally after a 6-h fast, and blood glucose was measured at 0, 15, 30, and 60 min.[37]

Statistical Analyses

Results are expressed as means ± SEM. ANOVA with subsequent Scheffe test was used to determine the significance of differences in multiple comparisons. $P < 0.05$ was considered statistically significant.

ACKNOWLEDGMENTS

We are highly appreciative of Makiko Sera for excellent technical assistance.

DISCLOSURES

None.

REFERENCES

1. Lakka HM, Laaksonen DE, Lakka TA, Niskanen LK, Kumpusalo E, Tuomilehto J, Salonen JT: The metabolic syndrome and total and cardiovascular disease mortality in middle-aged men. *JAMA* 288: 2709–2716, 2002
2. Isomaa B, Almgren P, Tuomi T, Forsen B, Lahti K, Nissen M, Taskinen MR, Groop L: Cardiovascular morbidity and mortality associated with the metabolic syndrome. *Diabetes Care* 24: 683–689, 2001
3. Chen J, Muntner P, Hamm LL, Jones DW, Batuman V, Fonseca V, Whelton PK, He J: The metabolic syndrome and chronic kidney disease in US adults. *Ann Intern Med* 140: 167–174, 2004
4. Praga M: Obesity: A neglected culprit in renal disease. *Nephrol Dial Transplant* 17: 1157–1159, 2002
5. Abrass CK: Overview: Obesity—What does it have to do with kidney disease? *J Am Soc Nephrol* 15: 2768–2772, 2004
6. Bagby SP: Obesity-initiated metabolic syndrome and the kidney: A recipe for chronic kidney disease? *J Am Soc Nephrol* 15: 2775–2791, 2004
7. Wisse BE: The inflammatory syndrome: The role of adipose tissue cytokines in metabolic disorders linked to obesity. *J Am Soc Nephrol* 15: 2792–2800, 2004
8. El-Atat FA, Stas SN, McFarlane SI, Sowers JR: The relationship between hyperinsulinemia, hypertension and progressive renal disease. *J Am Soc Nephrol* 15: 2816–2827, 2004
9. Gin H, Rigalleau V, Aparicio M: Lipids, protein intake, and diabetic nephropathy. *Diabetes Metab* 26[Suppl 4]: 45–53, 2000
10. Bonnet F, Cooper ME: Potential influence of lipids in diabetic nephropathy: Insights from experimental data and clinical studies. *Diabetes Metab* 26: 254–264, 2000
11. Sun L, Halaihel N, Zhang W, Rogers T, Levi M: Role of sterol regulatory element-binding protein 1 in regulation of renal lipid metabolism and glomerulosclerosis in diabetes mellitus. *J Biol Chem* 277: 18919–18927, 2002
12. Spencer MW, Muhlfeld AS, Segerer S, Hudkins KL, Kirk E, LeBoeuf RC, Alpers CE: Hyperglycemia and hyperlipidemia act synergistically to induce renal disease in LDL receptor-deficient BALB mice. *Am J Nephrol* 24: 20–31, 2004
13. Jiang T, Wang Z, Proctor G, Moskowitz S, Liebman SE, Rogers T, Lucia MS, Li J, Levi M: Diet-induced obesity in C57BL/6J mice causes increased renal lipid accumulation and glomerulosclerosis via a sterol regulatory element-binding protein-1c-dependent pathway. *J Biol Chem* 280: 32317–32325, 2005
14. Jump DB, Botolin D, Wang Y, Xu J, Christian B, Demeure O: Fatty acid regulation of hepatic gene transcription. *J Nutr* 135: 2503–2506, 2005
15. Jeukendrup AE: Regulation of fat metabolism in skeletal muscle. *Ann N Y Acad Sci* 967: 217–235, 2002
16. Reddy JK, Rao MS: Lipid metabolism and liver inflammation. II. Fatty liver disease and fatty acid oxidation. *Am J Physiol Gastrointest Liver Physiol* 290: G852–G858, 2006
17. Horton JD, Goldstein JL, Brown MS: SREBPs: Activators of the complete program of cholesterol and fatty acid synthesis in the liver. *J Clin Invest* 109: 1125–1131, 2002
18. Kelley DE, Simoneau JA: Impaired free fatty acid utilization by skeletal muscle in non-insulin-dependent diabetes mellitus. *J Clin Invest* 94: 2349–2356, 1994
19. Pan DA, Lillioja S, Kriketos AD, Milner MR, Baur LA, Bogardus C, Jenkins AB, Storlien LH: Skeletal muscle triglyceride levels are inversely related to insulin action. *Diabetes* 46: 983–988, 1997
20. Yamauchi T, Kamon J, Waki H, Murakami K, Motojima K, Komeda K, Ide T, Kubota N, Terauchi Y, Tobe K, Miki H, Tsuchida A, Akanuma Y,

Nagai R, Kimura S, Kadowaki T: The mechanisms by which both heterozygous peroxisome proliferator-activated receptor gamma (PPARgamma) deficiency and PPARgamma agonist improve insulin resistance. *J Biol Chem* 276: 41245–41254, 2001
21. Kubota N, Terauchi Y, Miki H, Tamemoto H, Yamauchi T, Komeda K, Satoh S, Nakano R, Ishii C, Sugiyama T, Eto K, Tsubamoto Y, Okuno A, Murakami K, Sekihara H, Hasegawa G, Naito M, Toyoshima Y, Tanaka S, Shiota K, Kitamura T, Fujita T, Ezaki O, Aizawa S, Kadowaki T, *et al.*: PPAR gamma mediates high-fat diet-induced adipocyte hypertrophy and insulin resistance. *Mol Cell* 4: 597–609, 1999
22. Rawson RB: The SREBP pathway: Insights from Insigs and insects. *Nat Rev Mol Cell Biol* 4: 631–640, 2003
23. Long YC, Zierath JR: AMP-activated protein kinase signaling in metabolic regulation. *J Clin Invest* 116: 1776–1783, 2006
24. Wei P, Lane PH, Lane JT, Padanilam BJ, Sansom SC: Glomerular structural and functional changes in a high-fat diet mouse model of early-stage type 2 diabetes. *Diabetologia* 47: 1541–1549, 2004
25. Wang Z, Jiang T, Li J, Proctor G, McManaman JL, Lucia S, Chua S, Levi M: Regulation of renal lipid metabolism, lipid accumulation, and glomerulosclerosis in FVBdb/db mice with type 2 diabetes. *Diabetes* 54: 2328–2335, 2005
26. Jiang T, Liebman SE, Lucia MS, Li J, Levi M: Role of altered renal lipid metabolism and the sterol regulatory element binding proteins in the pathogenesis of age-related renal disease. *Kidney Int* 68: 2608–2620, 2005
27. Lefebvre P, Chinetti G, Fruchart JC, Staels B: Sorting out the roles of PPAR alpha in energy metabolism and vascular homeostasis. *J Clin Invest* 116: 571–580, 2006
28. Matsusue K, Haluzik M, Lambert G, Yim SH, Gavrilova O, Ward JM, Brewer B Jr, Reitman ML, Gonzalez FJ: Liver-specific disruption of PPARgamma in leptin-deficient mice improves fatty liver but aggravates diabetic phenotypes. *J Clin Invest* 111: 737–747, 2003
29. Jones JR, Barrick C, Kim KA, Lindner J, Blondeau B, Fujimoto Y, Shiota M, Kesterson RA, Kahn BB, Magnuson MA: Deletion of PPARgamma in adipose tissues of mice protects against high fat diet-induced obesity and insulin resistance. *Proc Natl Acad Sci U S A* 102: 6207–6212, 2005
30. Isshiki K, Haneda M, Koya D, Maeda S, Sugimoto T, Kikkawa R: Thiazolidinedione compounds ameliorate glomerular dysfunction independent of their insulin-sensitizing action in diabetic rats. *Diabetes* 49: 1022–1032, 2000
31. Guo B, Koya D, Isono M, Sugimoto T, Kashiwagi A, Haneda M: Peroxisome proliferator-activated receptor-gamma ligands inhibit TGF-beta 1-induced fibronectin expression in glomerular mesangial cells. *Diabetes* 53: 200–208, 2004
32. Sarafidis PA, Bakris GL: Protection of the kidney by thiazolidinediones: An assessment from bench to bedside. *Kidney Int* 70: 1223–1233, 2006
33. Yu C, Markan K, Temple KA, Deplewski D, Brady MJ, Cohen RN: The nuclear receptor corepressors NCoR and SMRT decrease peroxisome proliferator-activated receptor gamma transcriptional activity and repress 3T3–L1 adipogenesis. *J Biol Chem* 280: 13600–13605, 2005
34. Cohen RN: Nuclear receptor corepressors and PPARgamma. *Nucl Recept Signal* 4: e003, 2006
35. Bligh EG, Dyer WJ: A rapid method of total lipid extraction and purification. *Can J Biochem Physiol* 37: 911–917, 1959
36. Koya D, Haneda M, Nakagawa H, Isshiki K, Sato H, Maeda S, Sugimoto T, Yasuda H, Kashiwagi A, Ways DK, King GL, Kikkawa R: Amelioration of accelerated diabetic mesangial expansion by treatment with a PKC beta inhibitor in diabetic db/db mice, a rodent model for type 2 diabetes. *FASEB J* 14: 439–447, 2000
37. Chin M, Isono M, Isshiki K, Araki S, Sugimoto T, Guo B, Sato H, Haneda M, Kashiwagi A, Koya D: Estrogen and raloxifene, a selective estrogen receptor modulator, ameliorate renal damage in db/db mice. *Am J Pathol* 166: 1629–1636, 2005

FEBS Letters 582 (2008) 74–80

Minireview

The physiological and pathophysiological role of adiponectin and adiponectin receptors in the peripheral tissues and CNS

Takashi Kadowaki[a,b,*], Toshimasa Yamauchi[a,c], Naoto Kubota[a,b,c]

[a] *Department of Metabolic Diseases, Graduate School of Medicine, University of Tokyo, Tokyo, Japan*
[b] *Division of Applied Nutrition, National Institute of Health and Nutrition, Tokyo, Japan*
[c] *Department of Integrated Molecular Science on Metabolic Diseases, Graduate School of Medicine, University of Tokyo, Tokyo, Japan*

Received 21 September 2007; revised 23 November 2007; accepted 23 November 2007

Available online 3 December 2007

Edited by Peter Tontonoz and Laszlo Nagy

Abstract Adiponectin is an abundantly expressed adipokine in adipose tissue and has direct insulin sensitizing activity. A decrease in the circulating levels of adiponectin by interactions between genetic factors and environmental factors causing obesity has been shown to contribute to the development of insulin resistance, type 2 diabetes, metabolic syndrome and atherosclerosis. In addition to its insulin sensitizing actions, adiponectin has central actions in the regulation of energy homeostasis. Adiponectin enhances AMP-activated protein kinase activity in the arcuate hypothalamus via its receptor AdipoR1 to stimulate food intake and decreases energy expenditure. We propose a hypothesis on the physiological role of adiponectin: a starvation gene in the course of evolution by promoting fat storage on facing the loss of adiposity.

Keywords: Adiponectin; Adipoectin receptor; Metabolic syndrome; AMP-activated protein kinase (AMPK); Energy homeostasis; Starvation gene

1. Introduction

Obesity-linked insulin resistance is a key feature of type 2 diabetes, metabolic syndrome and cardiovascular diseases [32,29,11]. White adipose tissue (WAT) has been recognized as an important endocrine organ that secretes a number of biologically active 'adipokines' [10,42,34,24]. Dysregulation of these adipokines have been shown to affect insulin sensitivity through modulation of insulin signaling pathway such as phosphorylation of the insulin receptor substrate (IRS) proteins (e.g. IRS1 and IRS2) [10] and the molecules involved in glucose and lipid metabolism in the peripheral tissues such as liver and skeletal muscle [33]. Of these adipokines, adiponectin has recently attracted much attention because of its antidiabetic and antiatherogenic effects [39,3,4,8,12,30,13]. Indeed, a decrease in the circulating levels of adiponectin by interactions between genetic factors and environmental factors causing obesity has been shown to contribute to the development of insulin resistance, type 2 diabetes, the metabolic syndrome and atherosclerosis (Fig. 1) [12,13].

In addition to these peripheral actions, adipokines have also been reported to have central actions in the regulation of energy homeostasis. Leptin binds is known to bind to the leptin receptor (LRb) in the hypothalamus and activates JAK2 (Janus kinase 2)-STAT3 (signal transducer and activator of transcription 3) and phosphatidylinositol-3 kinase (PI3K) pathway to increase metabolic rate and sympathetic tone and suppress feeding, thereby decreasing body weight [7]. Moreover, leptin has been reported to inhibit AMP-activated protein kinase (AMPK) activity in the hypothalamus and suppress food intake [28]. Recently, like leptin, adiponectin has been demonstrated to play an important role in the central nervous system (CNS). Adiponectin was shown to be present in the CSF of rodents [31,22] and human [23,19,6] and to enter the CSF from the circulation [31,22]. Moreover, the adiponectin receptors adipoR1 and adipoR2 [40] were found to be expressed in the hypothalamus and brain endothelial cells [35,22].

In this Review, we outline the recent progress in research on the physiological and pathophysiological role of adiponectin and adiponectin receptors in the peripheral tissues and CNS. Since the length of this Review is limited, we recommend that readers also consult other recent reviews on adiponectin research [4,12,13,30].

2. Cloning, function, and regulation of adiponectin receptors

In order to understand the molecular mechanism of adiponectin action, we isolated cDNA for human adiponectin receptors [40]. The cDNA encoded a protein designated adiponectin receptor 1 (AdipoR1) [40]. This protein is structurally conserved from yeast to humans (especially in the 7 transmembrane domains). Interestingly, the yeast homologue (YOL002c) plays a key role in metabolic pathways that regulate lipid metabolism, such as fatty acid oxidation [14]. Moreover, we found a gene that was significantly homologous (67% amino acid identity) with AdipoR1, which was termed AdipoR2 [40]. AdipoR1 is ubiquitously expressed, including in skeletal muscle and liver, whereas AdipoR2 is most abundantly expressed in the liver. AdipoR1 and AdipoR2 appear to be integral membrane proteins; the N-terminus is internal and the C-terminus is external-opposite to the topology of

*Corresponding author. Address: Department of Metabolic Diseases, Graduate School of Medicine, University of Tokyo, Tokyo, Japan.
E-mail address: kadowaki-3im@h.u-tokyo.ac.jp (T. Kadowaki).

0014-5793/$32.00
doi:10.1016/j.febslet.2007.11.070

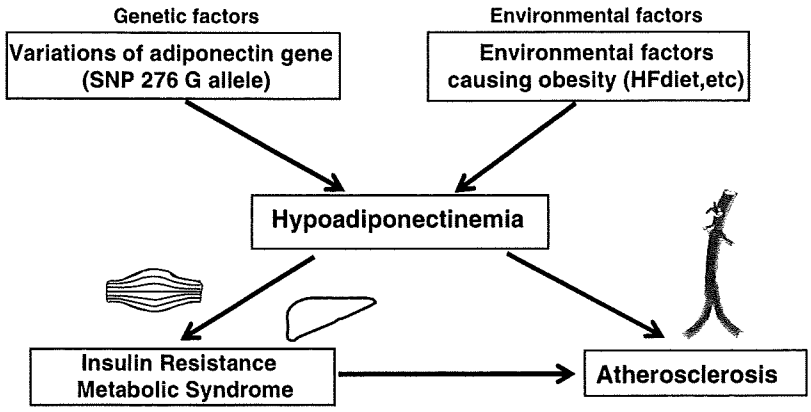

Fig. 1. Decrease in the circulating levels of adiponectin by interactions between genetic factors and environmental factors causing obesity has been shown to contribute to the development of insulin resistance, type 2 diabetes, the metabolic syndrome and atherosclerosis [12].

all other reported G protein-coupled receptors (GPCRs) [40]. Expression of AdipoR1 and AdipoR2 or suppression of AdipoR1 and AdipoR2 expression supports our conclusion that AdipoR1 and AdipoR2 serve as receptors for globular and full-length adiponectin and mediate increased AMPK, PPARα and p38 MAP kinase activities as well as fatty-acid oxidation and glucose uptake by adiponectin.

Recently, a two-hybrid study revealed that the C-terminal extracellular domain of AdipoR1 interacted with adiponectin, whereas the N-terminal cytoplasmic domain of AdipoR1 interacted with APPL (adaptor protein containing pleckstrin homology domain, phosphotyrosine-binding domain, and leucine zipper motif) [26]. Moreover, interaction of APPL with AdipoR1 in mammalian cells was stimulated by adiponectin binding, and this interaction appeared to play an important role in adiponectin-mediated AMPK activation and downstream effects [26].The expression levels of both AdipoR1 and AdipoR2 were significantly decreased in insulin-resistant *ob/ob* mice, probably in part because of obesity-linked hyperinsulinaemia [36]. Moreover, adiponectin-induced activation of AMPK was significantly decreased, for example, in the skeletal muscle of *ob/ob* mice, suggesting that adiponectin resistance is present in *ob/ob* mice [36]. Thus, obesity decreases not only plasma adiponectin levels but also AdipoR1/R2 expression, thereby causing adiponectin resistance and leading to insulin resistance, which in turn aggravates hyperinsulinaemia, forming a 'vicious cycle' [36].

3. Expression of adiponectin receptors in the liver ameliorated diabetes

Consistent with the data in *ob/ob* mice, expression levels of *AdipoR1* or *AdipoR2* were decreased to approximately 65% or 55%, respectively, in the liver of *db/db* mice as compared with wild-type mice. To determine the role of decreased expression levels of AdipoRs in the development of the insulin resistance and diabetes observed in obese mice, we studied the effects of adenovirus-mediated restoration of AdipoR1 expression in *db/db* mice. In fact, adenovirus-mediated overexpression of AdipoR1 or AdipoR2 in the liver of *db/db* mice significantly improved insulin resistance and diabetes in *db/db* mice [41].

3.1. *AdipoR1 increases AMPK activation by adiponectin in liver*

Expression of AdipoR1 resulted in significantly increased activation of AMPK in the liver by adiponectin, whereas expression of AdipoR2 did not. Activation of AMPK in the liver has been reported to reduce the expression of genes encoding hepatic gluconeogenic enzymes such as glucose-6-phosphatase (*G6pc*) and phosphoenolpyruvate carboxykinase 1 (*Pck1*) [25] as well as genes encoding molecules involved in lipogenesis such as sterol regulatory element binding protein 1c (*Srebf1*) [37]. In fact, expression of AdipoR1 significantly decreased the expressions of *G6pc*, *Pck1* and *Srebf1* in the liver of *db/db* mice, which may be among mechanisms by which restoration of AdipoR1 in the liver reduced endogenous glucose production (EGP), apparently increased glucose infusion rate (GIR) and improved diabetes [41]. In contrast, expression of AdipoR2 had little effects on the expression levels of *G6pc*, *Pck1* or *Srebf1*. These results suggested that AdipoR1 may be more involved in the activation of AMPK by adiponectin than AdipoR2 in liver in vivo [41].

3.2. *AdipoR2 increases PPARα target genes in liver*

Expression of AdipoR2 significantly increased the expression of genes encoding molecules involved in glucose uptake such as glucokinase (*Gck*) [27], unlike the molecules involved in gluconeogenesis, which appeared to be one possible mechanism by which AdipoR2 expression in the liver apparently increased GIR and improved diabetes. On the other hand, expression of AdipoR1 had little effect on the expression levels of *Gck*. Expression of AdipoR2 in liver of *db/db* mice increased PPARα (*Ppara*) itself [41] and its target genes [16] such as *Acox1* (acyl-CoA oxidase) and *Ucp2* (uncoupling protein 2), whereas expression of AdipoR1 in liver of *db/db* mice had little effects on PPARα itself and its target genes such as *Acox1 and Ucp2*. These observations suggested that AdipoR2 may be more involved in activation of the PPARα pathways than AdipoR1. Adenovirus-mediated expression of AdipoR1 or AdipoR2 in the liver of *db/db* mice significantly increased fatty-acid oxidation, and tended to decrease hepatic triglyceride content, which may be one mechanism by which expression of AdipoR1 or AdipoR2 in the liver improved insulin resistance and diabetes [41] (Fig. 2). The present data suggest that down-regulation of AdipoR1 and AdipoR2 in obesity plays causal roles, at least

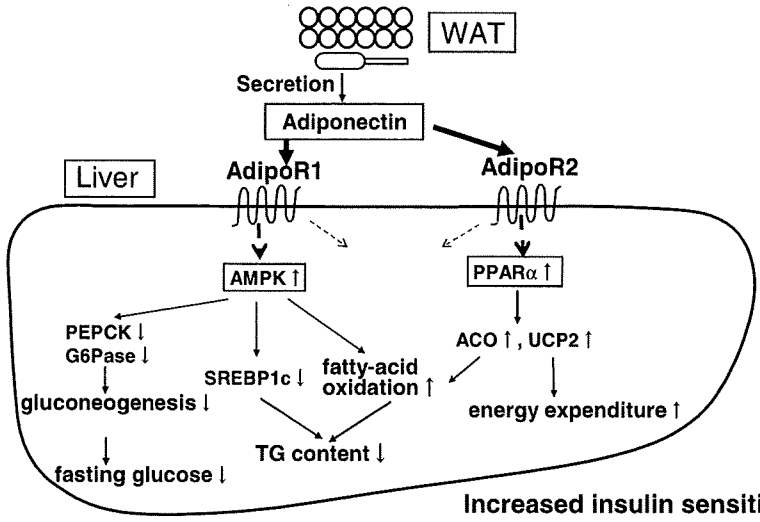

Fig. 2. AdipoR1 appears to mediate its biological effects via AMPK, whereas AdipoR2 appears to mediate them via PPARα.

in part, in the development of insulin resistance and diabetes.

4. AdipoR1 and AdipoR2 serve as the major adiponectin receptor in vivo

We generated *AdipoR1* knockout mice, *AdipoR2* knockout mice and *AdipoR1/R2* double knockout mice [41]. *AdipoR1* knockout mice showed significantly impaired glucose tolerance and insulin resistance. EGP was significantly increased and GIR was significantly decreased in *AdipoR1* knockout mice as compared with the wild-type mice. These observations indicate increased hepatic glucose production and insulin resistance in liver of *AdipoR1* knockout mice. Although glucose intolerance was not observed in *AdipoR2* knockout mice, plasma insulin levels were found to be significantly higher in the *AdipoR2* knockout mice than in the wild-type mice, suggesting the presence of insulin resistance in the *AdipoR2* knockout mice. In contrast to *AdipoR1* knockout mice, EGP was not significantly higher in *AdipoR2* knockout mice. However, GIR was significantly decreased, and Rd tended to be decreased in AdipoR2 knockout mice. AdipoR1/R2 double knockout mice exhibited significantly impaired glucose tolerance and insulin resistance. There is a significant elevation of the insulin resistance index in the AdipoR1/R2 double knockout mice compared to the AdipoR1 knockout mice, and this can be attributed to the contribution of the AdipoR2 deficiency. These findings provided the first direct evidence that AdipoR1 and AdipoR2 do indeed play important physiological roles in the regulation of insulin sensitivity in vivo. Liver is a major target of adiponectin action [3]. We detected no appreciable adiponectin specific binding activity in the hepatocytes from AdipoR1/R2 double knockout mice, indicating undetectable levels of functional adiponectin receptors in hepatocytes from AdipoR1/R2 double knockout mice. Consistent with this, glucose lowering effect of adiponectin was completely abrogated in AdipoR1/R2 double knockout mice. Thus, AdipoR1 and AdipoR2 are the major adiponectin receptors in vivo, which mediate the major, if not the entire, part of adiponectin binding and adiponectin actions.

5. Adiponectin receptors are present in the hypothalamus, and adiponectin enters the CSF from the circulation

Since the end of the 19th century, several efforts have been made to determine the CNS' role in the regulation of energy metabolism. In 1953, Gordon Kennedy proposed a "lipostat theory" that body fat content is maintained by factors secreted from adipose tissue, as a result of feedback signals arising from the fat depots that are sensed by the brain [15]. The hormone leptin circulates in proportion to body fat [2]. Leptin informs the CNS that adipose stores are expanding and prevents from accumulating excessive fat storage through coordinated regulation of feeding, metabolism, the autonomic nervous system and body energy balance. In contrast, no adipokine has been identified that promotes fat accumulation when energy balance is disrupted.

AdipoR1 and AdipoR2 [40], were found to be abundantly expressed in the hypothalamus, and their expression levels were comparable to those in the liver. In situ hybridization analysis revealed the expressions of AdipoR1 and AdipoR2 as well as the leptin receptor in the ARH. Immunohistochemical analysis revealed colocalization of AdipoR1 and the leptin receptor in the ARH of C57BL/6 mice. Adiponectin was detected in the CSF of C57BL/6 mice at approximately 1/4000th of its concentration in the serum; it was also detected in the CSF of adiponectin knockout mice [20,21] after intravenous (i.v.) injection of full-length adiponectin administered to raise the serum adiponectin levels in these mice to approximately the same levels as in wild-type mice. These findings indicate that adiponectin does indeed enter the CSF from the circulation [22]. Adiponectin is known to exist in three forms, namely, trimers, hexamers, and HMW multimers, in the serum of wild-type mice. Interestingly, unlike in the serum, only trimers and hexamers, and not HMW multimers, were found in the CSF of the wild-type mice. In adiponectin knockout mice, after i.v. injection of full-length adiponectin, all three forms, i.e., trimers, hexamers, and HMW multimers, were found in the serum, while only trimers and hexamers, and not HMW multimers, were found in the CSF. These data indicate that the distribution of the multimeric forms of adiponectin in the CSF differs from that in the serum [22]. In wild-type mice,

while plasma levels of glucose and insulin and serum levels of leptin increased significantly after refeeding, serum and CSF adiponectin levels decreased significantly. In addition, the expression of AdipoR1 in the ARH decreased significantly after refeeding, whereas that of AdipoR2 remained unchanged.

6. Adiponectin increases AMPK activity in the ARH via AdipoR1 to stimulate food intake

In view of the increases in adiponectin concentrations in the serum and CSF and the increases in the AdipoR1 expression level in the ARH under fasting conditions, adiponectin signals may be involved in the stimulation of food intake. It has been suggested that adiponectin is an orexigenic hormone and that it may stimulate the phosphorylation of AMPK and acetyl-CoA carboxylase (ACC), downstream of AMPK, in the hypothalamus [1,9,5,38]. Phosphorylation of AMPK and ACC was suppressed after refeeding [1,28,38]. Administration of adiponectin increased the phosphorylation of AMPK and ACC. Next, we investigated whether the enhanced AMPK activation by adiponectin was mediated by the adiponectin receptors expressed in the ARH by injecting adeno-AdipoR1 siRNA or adeno-AdipoR2 siRNA into the ARH, using adeno-LacZ as a control. The phosphorylation of AMPK and ACC in the ARH was significantly suppressed in the adeno-AdipoR1 siRNA-treated mice as compared with the adeno-LacZ-treated mice under fasting conditions. After refeeding, phosphorylation of AMPK and ACC was also suppressed in the control group treated with adeno-LacZ, and this was reversed by the administration of adiponectin. However, in the animals in which AdipoR1 expression in the ARH was decreased by treatment with AdipoR1 siRNA, adiponectin failed to reverse the suppression of AMPK and ACC phosphorylation observed after refeeding. On the other hand, when AdipoR2 expression in the ARH was reduced by the administration of AdipoR2 siRNA, the suppression of AMPK and ACC phosphorylation after refeeding was still reversed by adiponectin. These findings suggest that adiponectin directly activates AMPK in the ARH via AdipoR1, but not AdipoR2. Since increased AMPK activity in the ARH has been shown to stimulate food intake [9,28,5], we then investigated the effect of adiponectin on food intake. Food intake after refeeding was significantly lower than after fasting, as the AMPK and ACC phosphorylation levels decreased. Adiponectin injection significantly increased food intake after refeeding, as the AMPK and ACC phosphorylation levels increased. In the mice in which AdipoR1 expression in the ARH was decreased by treatment with AdipoR1 siRNA, the stimulation of food intake by adiponectin injection was blunted. On the other hand, in the mice in which AdipoR2 expression in the ARH was decreased by treatment with AdipoR2 siRNA, no such blunting of the effect of adiponectin injection was observed. These findings suggest that adiponectin stimulates food intake via AdipoR1 in the ARH. Next, in order to investigate whether the stimulation of food intake induced by adiponectin is actually mediated by AMPK, dominant-negative AMPK (D/N-AMPK) was expressed in the ARH, and the amount of food intake was measured. In the control group treated with LacZ, the amount of food consumed after adiponectin injection was significantly higher than after saline injection. In contrast, in the group treated with D/N-AMPK, the stimulation of food intake by the adiponectin injection was blunted, suggesting that adiponectin has a central action of stimulating food intake by activating AMPK in the ARH. In addition to regulating food intake, AMPK in the hypothalamus is also thought to regulate energy expenditure [9,5,17]. Examination of the effect of adiponectin on energy expenditure revealed that oxygen consumption was significantly decreased by adiponectin. Consistent with these findings, expression of uncoupling protein 1 (UCP1) in brown adipose tissue (BAT) was significantly decreased after i.v. injection of adiponectin. We then administered the hexameric form of adiponectin, the predominant form in the CSF, directly into the lateral cerebral ventricles and examined the direct effects of adiponectin in order to rule out the possibility that the actions of adiponectin on the peripheral organs participate in the AMPK activation in the ARH and stimulation of food intake. The suppression of AMPK and ACC phosphorylation after refeeding was indeed reversed by intracerebroventricular (i.c.v.) administration of the hexameric form of adiponectin. Intracerebroventricular injection of the hexameric form of adiponectin also significantly stimulated food intake after refeeding, along with increasing the AMPK and ACC phosphorylation levels. Moreover, oxygen consumption was significantly decreased following i.c.v. injection of the hexameric form of adiponectin. Intravenous injection of adiponectin decreased energy expenditure and UCP1 expression in BAT. Taken together, these findings indicate that adiponectin directly regulates AMPK activity in the ARH and food intake.

Scherer's group has generated adiponectin-transgenic ob/ob mice that show serum adiponectin levels 2–3-fold higher than ob/ob mice [18]. These mice also show markedly increased body weight due to decreased energy expenditure, as manifested by lower body temperature and lower oxygen consumption, consistent with our observations that adiponectin decreases energy expenditure.

7. Adiponectin knockout mice exhibit decreased AMPK activity in the ARH, increased oxygen consumption, and greater loss of fat during fasting

In order to further elucidate the physiological role of adiponectin in the CNS, we investigated the effects of adiponectin deficiency on AMPK activity, food intake, and energy homeostasis in adiponectin knockout mice. AMPK phosphorylation in the ARH was significantly suppressed in adiponectin knockout mice after fasting. Expression of neuropeptide Y (NPY) in the ARH after fasting was also significantly lower in adiponectin knockout mice, while the expression of pro-opiomelanocortin (POMC) in the ARH was increased after fasting in these mice. Consistent with the decreased AMPK activity and decreased NPY expression in the ARH, adiponectin knockout mice consumed significantly more oxygen than their wild-type littermates under fasting conditions. Expression of UCP1 in BAT was significantly increased in adiponectin knockout mice as compared with wild-type mice. Moreover, despite the adiponectin deficiency, AMPK phosphorylation in skeletal muscle was significantly increased in adiponectin knockout mice compared to their wild-type littermates. These increases in UCP1 expression and AMPK phosphorylation, which may account for the increased energy expenditure in adiponectin knockout mice, cannot be explained by the peripheral actions of adipo-

nectin but may presumably be explainable by its central actions. Despite the similar body weight of wild-type and adiponectin knockout mice, body fat mass, as measured by dual energy X-ray absorptiometry (DEXA), was significantly lower in adiponectin knockout mice than in wild-type mice. The reduction in visceral and subcutaneous fat mass after fasting was greater in adiponectin knockout mice than in wild-type mice.

8. Adiponectin knockout mice exhibit reduced food intake and increased oxygen consumption and appear to be protected from high-fat diet-induced obesity

Adiponectin knockout mice were found to be more resistant to high-fat diet (HFD)-induced obesity than wild-type mice. The visceral WAT mass and subcutaneous WAT mass were both significantly smaller in adiponectin knockout mice fed a HFD. Histological analysis of WAT and quantitation of adipocyte size in the mice revealed significantly smaller adipocytes in adiponectin knockout mice than in wild-type mice. Additionally, after 2 weeks of HFD, when the two groups were indistinguishable by body weight, we examined AMPK and ACC phosphorylation status, AdipoR1 and AdipoR2 expression, food intake, and oxygen consumption in the two groups. AMPK and ACC phosphorylation in the ARH was significantly suppressed in adiponectin knockout mice after fasting, although the expression levels of AdipoR1 and AdipoR2 in the ARH were not significantly different between the two genotypes. Daily food intake was significantly lower in adiponectin knockout mice than in wild-type mice, and oxygen consumption was significantly greater.

9. Physiological and pathophysiological roles of adiponectin

These findings have brought new insights on adiponectin as an appetite stimulator, longer-term fat modulator, and a starvation signal. We propose a hypothesis that adiponectin regulates food intake in coordination with leptin. Under fasting conditions, the adiponectin signal in the ARH increases; consequently, hypothalamic AMPK is activated, which stimulates food intake. After food consumption, on the other hand, the leptin signal in the ARH increases; consequently, hypothalamic AMPK activity decreases, resulting in reduced food intake. Thus, the leptin signal is regulated inversely in relation to adiponectin signal in the hypothalamus. Adiponectin enhances hypothalamic AMPK activity and food intake, as opposed to the action of leptin.

In addition to the regulation of food intake, adiponectin and leptin may also participate in the maintenance of energy homeostasis. Several gut-derived hormones, such as ghrelin and insulin, have been discovered as the modulator of energy balance, which primarily act on appetite. Adipokines appear to be also involved in this; they mainly regulate body fat mass as the long-term modulator of energy balance. On facing the loss of adiposity, the adiponectin signal increases and leptin signal decreases in the ARH; consequently, hypothalamic AMPK is activated, which suppresses energy expenditure, promoting fat storage. On facing the excessive adiposity, on the other hand, the adiponectin signal decreases and the leptin signal increases in the ARH; consequently, hypothalamic AMPK activity decreases that stimulates energy expenditure, inhibiting fat accumulation. Thus the fundamental roles of leptin and adiponectin seem to be to preserve an adequate fat reserve: leptin acts as a satiety signal, and adiponectin acts as a starvation signal. These observations support the lipostat theory, and adiponectin is the first-identified adipokine that contributes to fat accumulation in response to depletion of adiposity (Fig. 3).

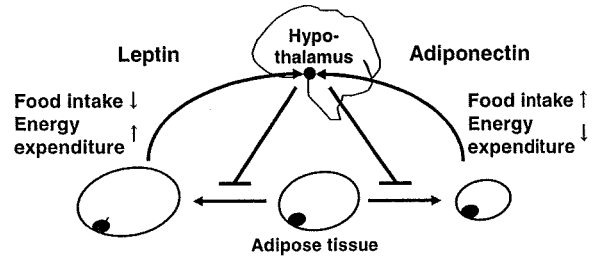

Fig. 3. Body fat content is maintained by factors secreted from adipose tissue, as a result of feedback signals arising from the fat depots that are sensed by the brain.

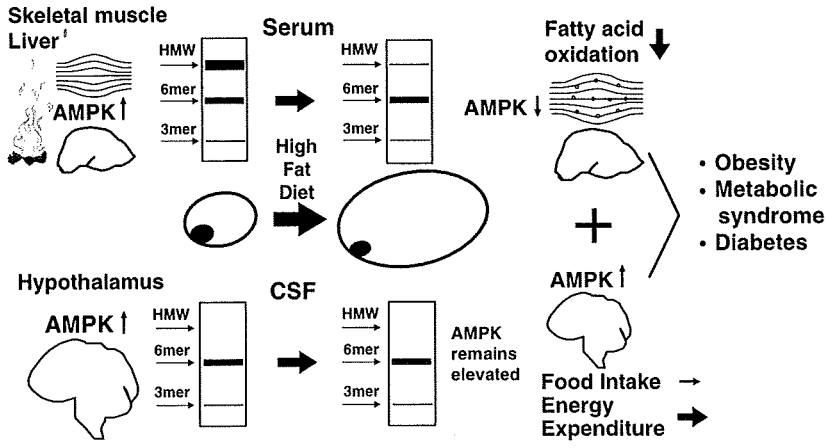

Fig. 4. Under a high-fat diet, adiponectin-induced AMPK in the brain remains elevated, while that in the liver and muscle is markedly attenuated, thus further worsening obesity, metabolic syndrome and type 2 diabetes.

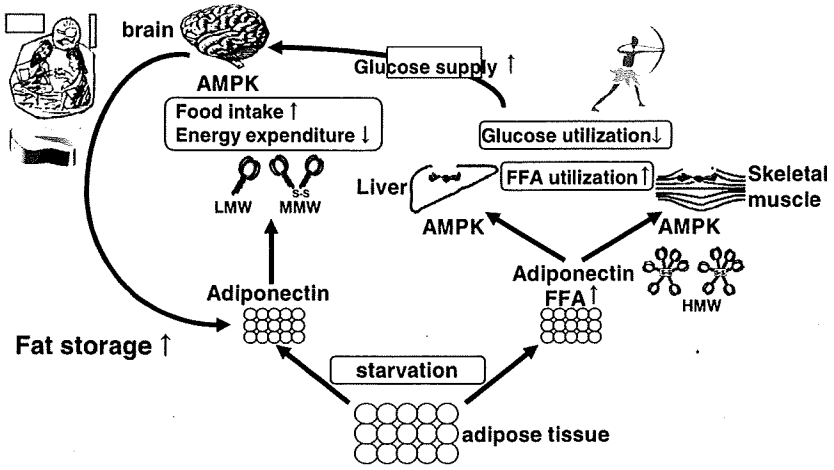

Fig. 5. Adiponectin serves as a starvation gene. Adiponectin inhibits energy expenditure, promotes food intake centrally, and stimulates FFA utilization in peripheral tissues.

Once this energy regulation is disrupted, obesity begins to develop. Under an excessive fat reserve, serum adiponectin levels are decreased. The HMW form of adiponectin is known to be most active [13] and does not enter the CSF [23,22]. Under an obese condition, serum adiponectin levels, especially of active HMW multimers, are reported to decrease in an obese individual and murine models, which decreases muscle and hepatic AMPK activity and fatty acid combustion, exacerbating insulin resistance. In the CNS, on the other hand, although a HMW form of adiponectin in serum decreases under an obese condition, trimers and hexamers are present, maintaining the serum adiponectin levels relatively stable in the CSF. Thus, hypothalamic AMPK activity is not suppressed, not decreasing food intake and energy expenditure. This results in worsening obesity, metabolic syndrome and type 2 diabetes (Fig. 4).

Lastly, let us consider the role of adiponectin in the history. During the course of evolution, starvation signals were essential for the survival of an organism. Adiponectin levels were likely to be high under the scarce fat reserve of starvation. Trimeric and hexameric forms of adiponectin would increase appetite by affecting the brain to decrease energy expenditure and to promote fat accumulation. The HMW form of adiponectin was likely to derive energy for survival from combusting (adipocyte-secreted) FFA in the liver and skeletal muscle. The increase in peripheral fatty acid combustion may have contributed to the preferential supply of glucose to the brain. Adiponectin may have played an important role as an starvation gene (Fig. 5). This may explain why adiponectin receptors existed earlier than leptin receptors and have been conserved from yeast to humans [14].

References

[1] Andersson, U., Filipsson, K., Abbott, C.R., et al. (2004) AMP-activated protein kinase plays a role in the control of food intake. J. Biol. Chem. 279, 12005–12008.
[2] Benoit, S.C., Clegg, D.J., Seeley, R.J., et al. (2004) Insulin and leptin as adiposity signals. Recent Prog. Horm. Res. 59, 267–285.
[3] Berg, A.H., Combs, T.P., Du, X., et al. (2001) The adipocyte-secreted protein Acrp30 enhances hepatic insulin action. Nat. Med. 7, 947–953.
[4] Berg, A.H. and Scherer, P.E. (2005) Adipose tissue, inflammation, and cardiovascular disease. Circ. Res. 96, 939–949.
[5] Carling, D. (2005) AMP-activated protein kinase: balancing the scales. Biochimie 87, 87–91.
[6] Ebinuma, H., Miida, T., Yamauchi, T., Hada, Y., Hara, K., Kubota, N. and Kadowaki, T. (2007) Improved ELISA for selective measurement of adiponectin multimers and identification of adiponectin in human cerebrospinal fluid. Clin. Chem. 53, 1541–1544.
[7] Friedman, J.M. (1996) Abnormal splicing of the leptin receptor in diabetic mice. Nature 379, 632–635.
[8] Fruebis, J., Tsao, T.S., Javorschi, S., et al. (2001) Proteolytic cleavage product of 30-kDa adipocyte complement-related protein increases fatty acid oxidation in muscle and causes weight loss in mice. Proc. Natl. Acad. Sci. USA 98, 2005–2010.
[9] Hardie, D.G. (2004) The AMP-activated protein kinase pathway-new players upstream and downstream. J. Cell Sci. 117, 5479–5487.
[10] Hotamisligil, G.S., Shargill, N.S. and Spiegelman, B.M. (1993) Adipose expression of tumor necrosis factor-alpha: direct role in obesity-linked insulin resistance. Science 259, 87–91.
[11] International Diabetes Federation. (2005) A new worldwide definition of the metabolic syndrome. <http://www.idf.org/home/index.cfm?unode=32EF2063-B966-468F-928CA5682A4E3910>.
[12] Kadowaki, T. and Yamauchi, T. (2005) Adiponectin and adiponectin receptors. Endocr. Rev. 26, 439–451.
[13] Kadowaki, T., Yamauchi, T., Kubota, N., Hara, K., Ueki, K. and Tobe, K. (2006) Adiponectin and adiponectin receptors in insulin resistance, diabetes, and the metabolic syndrome. J. Clin. Invest. 116, 1784–1792.
[14] Karpichev, I.V., Cornivelli, L. and Small, G.M. (2002) Multiple regulatory roles of a novel *Saccharomyces cerevisiae* protein, encoded by YOL002c, in lipid and phosphate metabolism. J. Biol. Chem. 277, 19609–19617.
[15] Kennedy, G.C. (1953) The role of depot fat in the hypothalamic control of food intake in the rat. Proc. R Soc. Lond. (Biol.) 140, 579–592.
[16] Kersten, S., Desvergne, B. and Wahli, W. (2000) Roles of PPARs in health and disease. Nature 405, 421–424.
[17] Kim, M.S. and Lee, K.U. (2005) Role of hypothalamic 50-AMP-activated protein kinase in the regulation of food intake and energy homeostasis. J. Mol. Med. 83, 514–520.
[18] Kim, J.Y., van de Wall, E., Laplante, M., et al. (2007) Obesity-associated improvements in metabolic profile through expansion of adipose tissue. J. Clin. Invest. 117, 2621–2637.
[19] Kos, K., Harte, A.L., da Silva, N.F., et al. (2007) Adiponectin and resistin in human cerebrospinal fluid and expression of adiponectin receptors in the human hypothalamus. J. Clin. Endocrinol. Metab. 92, 1129–1136.
[20] Kubota, N., Terauchi, Y., Yamauchi, T., et al. (2002) Disruption of adiponectin causes insulin resistance and neointimal formation. J. Biol. Chem. 277, 25863–25866.

[21] Kubota, N., Terauchi, Y., Kubota, T., et al. (2006) Pioglitazone ameliorates insulin resistance and diabetes by both adiponectin-dependent and -independent pathways. J. Biol. Chem. 281, 8748–8755.
[22] Kubota, N., Yano, W., Kubota, T., et al. (2007) Adiponectin stimulates AMP-activated protein kinase in the hypothalamus and increases food intake. Cell Metab. 6, 55–68.
[23] Kusminski, C.M., McTernan, P.G., Schraw, T., et al. (2007) Adiponectin complexes in human cerebrospinal fluid: distinct complex distribution from serum. Diabetologia 50, 634–642.
[24] Lazar, M.A. (2006) The humoral side of insulin resistance. Nat. Med. 12, 43–44.
[25] Lochhead, P.A., Salt, I.P., Walker, K.S., et al. (2000) 5-Amino-imidazole-4-carboxamide riboside mimics the effects of insulin on the expression of the 2 key gluconeogenic genes PEPCK and glucose-6-phosphatase. Diabetes 49, 896–903.
[26] Mao, X., Kikani, C.K., Riojas, R.A., et al. (2006) APPL1 binds to adiponectin receptors and mediates adiponectin signalling and function. Nat. Cell Biol. 8, 516–523.
[27] Matschinsky, F.M., Magnuson, M.A., Zelent, D., et al. (2006) The network of glucokinase-expressing cells in glucose homeostasis and the potential of glucokinase activators for diabetes therapy. Diabetes 55, 1–12.
[28] Minokoshi, Y., Alquier, T., Furukawa, N., et al. (2004) AMP-kinase regulates food intake by responding to hormonal and nutrient signals in the hypothalamus. Nature 428, 569–574.
[29] National Cholesterol Education Program. (2001) Executive summary of the third report of the national cholesterol education program (NCEP) expert panel on detection, evaluation, and treatment of high blood cholesterol in adults (Adult Treatment Panel III). JAMA 285:2486–2497.
[30] Okamoto, Y., Kihara, S., Funahashi, T., et al. (2006) Adiponectin: a key adipocytokine in metabolic syndrome. Clin. Sci. (Lond.) 110, 267–278.
[31] Qi, Y., Takahashi, N., Hileman, S.M., et al. (2004) Adiponectin acts in the brain to decrease body weight. Nat. Med. 10, 524–529.
[32] Reaven, G.M. (1998) Role of insulin resistance in human disease. Diabetes 37, 1595–1607.
[33] Shulman, G.I. (2000) Cellular mechanisms of insulin resistance. J. Clin. Invest. 106, 171–176.
[34] Steppan, C.M., Bailey, S.T., Bhat, S., et al. (2001) The hormone resistin links obesity to diabetes. Nature 409, 307–312.
[35] Spranger, J., Verma, S., Gohring, I., et al. (2006) Adiponectin does not cross the blood-brain barrier but modifies cytokine expression of brain endothelial cells. Diabetes 55, 141–147.
[36] Tsuchida, A., Yamauchi, T., Ito, Y., et al. (2004) Insulin/Foxo1 pathway regulates expression levels of adiponectin receptors and adiponectin sensitivity. J. Biol. Chem. 279, 30817–30822.
[37] Woods, A., Azzout-Marniche, D., Foretz, M., et al. (2000) Characterization of the role of AMPactivated protein kinase in the regulation of glucose-activated gene expression using constitutively active and dominant negative forms of the kinase. Mol. Cell Biol. 20, 6704–6711.
[38] Xue, B. and Kahn, B.B. (2006) AMPK integrates nutrient and hormonal signals to regulate food intake and energy balance through effects in the hypothalamus and peripheral tissues. J. Physiol. 574, 73–83.
[39] Yamauchi, T., Kamon, J., Waki, H., et al. (2001) The fat-derived hormone adiponectin reverses insulin resistance associated with both lipoatrophy and obesity. Nat. Med. 7, 941–946.
[40] Yamauchi, T., Kamon, J., Ito, Y., et al. (2003) Cloning of adiponectin receptors that mediate antidiabetic metabolic effects. Nature 423, 762–769.
[41] Yamauchi, T., Nio, Y., Maki, T., et al. (2007) Targeted disruption of AdipoR1 and AdipoR2 causes abrogation of adiponectin binding and metabolic actions. Nat. Med. 13, 332–339.
[42] Zhang, Y., Proenca, R., Maffei, M., Barone, M., Leopold, L. and Friedman, J.M. (1994) Positional cloning of the mouse obese gene and its human homologue. Nature 372, 425–432.

Diabetologia (2008) 51:827–835
DOI 10.1007/s00125-008-0944-9

ARTICLE

Adiponectin induces insulin secretion in vitro and in vivo at a low glucose concentration

M. Okamoto · M. Ohara-Imaizumi · N. Kubota · S. Hashimoto · K. Eto · T. Kanno · T. Kubota · M. Wakui · R. Nagai · M. Noda · S. Nagamatsu · T. Kadowaki

Received: 17 October 2007 / Accepted: 20 December 2007 / Published online: 28 March 2008

Abstract
Aims/hypothesis A decrease in plasma adiponectin levels has been shown to contribute to the development of diabetes. However, it remains uncertain whether adiponectin plays a role in the regulation of insulin secretion. In this study, we investigated whether adiponectin may be involved in the regulation of insulin secretion in vivo and in vitro.
Methods The effect of adiponectin on insulin secretion was measured in vitro and in vivo, along with the effects of adiponectin on ATP generation, membrane potentials, Ca^{2+} currents, cytosolic calcium concentration and state of 5′-AMP-activated protein kinase (AMPK). In addition, insulin granule transport was measured by membrane capacitance and total internal reflection fluorescence (TIRF) analysis.
Results Adiponectin significantly stimulated insulin secretion from pancreatic islets to approximately 2.3-fold the baseline value in the presence of a glucose concentration of 5.6 mmol/l. Although adiponectin had no effect on ATP generation, membrane potentials, Ca^{2+} currents, cytosolic calcium concentrations or activation status of AMPK, it caused a significant increase of membrane capacitance to approximately 2.3-fold the baseline value. TIRF analysis revealed that adiponectin induced a significant increase in the number of fusion events in mouse pancreatic beta cells under 5.6 mmol/l glucose loading, without affecting the status of previously docked granules. Moreover, intravenous injection of adiponectin significantly increased insulin secretion to approximately 1.6-fold of baseline in C57BL/6 mice.

M. Okamoto and M. Ohara-Imaizumi contributed equally to this study.

Electronic supplementary material The online version of this article (doi:10.1007/s00125-008-0944-9) contains supplementary material, which is available to authorised users.

M. Okamoto · N. Kubota · S. Hashimoto · K. Eto · T. Kubota · T. Kadowaki (✉)
Department of Metabolic Diseases, Graduate School of Medicine, University of Tokyo,
Hongo 7-3-1, Bunkyo-ku,
Tokyo 113-8655, Japan
e-mail: kadowaki-3im@h.u-tokyo.ac.jp

M. Ohara-Imaizumi · S. Nagamatsu
Department of Biochemistry,
Kyorin University School of Medicine,
Tokyo, Japan

N. Kubota · T. Kubota · T. Kadowaki
Division of Applied Nutrition,
National Institute of Health and Nutrition,
Tokyo, Japan

T. Kanno · M. Wakui
Department of Physiology,
Hirosaki University School of Medicine,
Hirosaki, Japan

R. Nagai
Department of Cardiovascular Medicine,
Graduate School of Medicine, University of Tokyo,
Tokyo, Japan

M. Noda
Department of Diabetes and Metabolic Medicine,
International Medical Center of Japan,
Tokyo, Japan

Conclusions/interpretation The above results indicate that adiponectin induces insulin secretion in vitro and in vivo.

Keywords Adiponectin · Beta cell · Capacitance · Fusion events · Insulin granules · Insulin secretion · Islet

Abbreviations

AICAR	5-amino-imidazole-4-carboxamide riboside
AMPK	5′-AMP-activated protein kinase
$[Ca^{2+}]_c$	cytosolic Ca^{2+} concentration
GFP	green fluorescent protein
LPS	lipopolysaccharide
TIRF	total internal reflection fluorescence

Introduction

The adipocyte-derived hormone adiponectin (also known as Acrp30, GBP28 or AdipoQ) [1–4] has been shown to play important roles in the regulation of glucose and lipid metabolism. Plasma adiponectin levels are reduced in obese and insulin-resistant humans and in animal models [2, 5, 6]. Adiponectin improves insulin sensitivity in muscle and liver by enhancing fatty acid oxidation via activation of 5′-AMP-activated protein kinase (AMPK) [7, 8] and peroxisome proliferator-activated receptor α [6, 9].

We previously demonstrated that adiponectin-deficient (*Adipo*$^{-/-}$) mice exhibit insulin resistance [10], but that after glucose loading the plasma insulin levels tended to be lower in *Adipo*$^{-/-}$ mice than in wild-type mice, suggesting that adiponectin may induce insulin secretion [10]. The adiponectin receptors ADIPOR1 and ADIPOR2 have recently been cloned [11] and identified in human and rat pancreatic beta cells [12]. Expression of the adiponectin receptors by INS-1 cells (a clonal rat beta cell line) has been found to increase following exposure to oleic acid, an unsaturated NEFA. Moreover, a previous study has suggested that adiponectin also exerts anti-apoptotic actions and that this protective function of adiponectin might serve to counteract autoimmune- and lipotoxicity-induced beta cell destruction [13]. However, it is still uncertain whether adiponectin plays a role in the regulation of insulin secretion. In this study we investigated whether adiponectin might be involved in the regulation of insulin secretion in vitro and in vivo.

Methods

Animals C57BL/6 mice were obtained from CLEA Japan (Tokyo, Japan). Male C57BL/6 mice (10 to 16 weeks old) were housed under a 12 h light–dark cycle and given free access to food. The animal care and experimental procedures were approved by the Animal Care Committee of the University of Tokyo.

RNA preparation and real-time quantitative PCR Total RNA was extracted from isolated islets using TRIzol reagent (Invitrogen, Carlsbad, CA, USA) according to the manufacturer's instructions. cDNA synthesis was performed using the SuperScript Preamplification System (Invitrogen), followed by TaqMan quantitative PCR (Applied Biosystems, Foster City, CA, USA; 50°C for 2 min and 95°C for 10 min, followed by 40 cycles of 95°C for 15 s and 60°C for 1 min) with an ABI Prism 7000 PCR instrument (Applied Biosystems) to amplify samples of the *Adipor1*, *Adipor2* and β-actin genes. The sequences of the primers and probes are described elsewhere [11].

Insulin secretion by islets Islets were isolated from 10- to 16-week-old C57BL/6 mice as described elsewhere [14]. In brief, after clamping the common bile duct at a point close to the duodenal outlet, 2.5 ml KRB (129 mmol/l NaCl, 4.8 mmol/l KCl, 1.2 mmol/l $MgSO_4$, 1.2 mmol/l KH_2PO_4, 2.5 mmol/l $CaCl_2$, 5 mmol/l $NaHCO_3$ and 10 mmol/l HEPES; pH 7.4) containing 4 mg/ml collagenase (Sigma, St Louis, MO, USA) was injected into the duct. Insulin release by the pancreatic islets was measured by static incubation with KRB containing 0.2% (wt/vol.) bovine serum albumin [15]. In the static incubation, batches of ten freshly isolated islets were preincubated at 37°C for 30 min in KRB containing 2.8 mmol/l glucose. The preincubation solutions were replaced with KRB containing test agents and the batches of islets were incubated at 37°C for 60 min. The insulin released in the supernatant fractions was then measured by radioimmunoassay (Biotrak; GE Healthcare, Chalfont St Giles, UK).

Generation of recombinant adiponectin Bacterially expressed murine full-length adiponectin was generated as described previously [7, 11]. The endotoxin content of the purified protein was determined using a Limulus Amebocyte Lysate Assay (Bio Whittaler, Walkersville, MD, USA). Mammalian adiponectin was purchased from Alexis Biochemicals (San Diego, CA, USA).

Glucose oxidation and fatty acid oxidation Glucose oxidation in the islets was evaluated by measuring the $^{14}CO_2$ generation from D-[6–^{14}C]glucose [16]. Batches of ten freshly isolated islets were incubated at 37°C for 60 min in KRB containing 29.6 kBq D-[6–^{14}C]glucose and 5.6 or 22.2 mmol/l glucose with and without 10 μg/ml adiponectin. For fatty acid oxidation, batches of ten freshly isolated islets were incubated at 37°C for 60 min in KRB containing 25.9 kBq [U-^{14}C]palmitic acid, 1 mmol/l carnitine, and 5.6 or

22.2 mmol/l glucose with and without 10 μg/ml adiponectin. The $^{14}CO_2$ produced was volatilised by adding HCl, captured with Solvable (Packard Instrument Company, Meriden, CT, USA) and measured by liquid scintillation counting.

ATP and cAMP content The ATP and cAMP contents of the islets were determined as described previously [17]. Briefly, batches of ten islets were incubated at 37°C for 60 min in KRB containing 5.6 mmol/l glucose with and without 10 μg/ml adiponectin. Incubation was stopped by the addition of ice-cold $HClO_4$ and the islets were homogenised by sonication. The lysates were neutralised by the addition of NaOH. The ATP content and cAMP content of the supernatant fraction were measured using a bioluminescent assay kit (Sigma) and an enzyme-linked immunoassay kit (GE Healthcare), respectively.

Electrical recordings Electrophysiological experiments on the islets were performed using cells in situ in intact pancreatic islets. The islets were washed extensively in collagenase-free solution and then maintained in a short-term tissue culture (<24 h) in RPMI 1640 containing 10% (vol./vol.) fetal calf serum supplemented with 100 μg/ml streptomycin and 100 IU/ml penicillin.

To establish the whole-cell mode, the amphotericin B-perforated patch-clamp technique was used. The membrane potential and the current of superficial cells in the intact pancreatic islets were recorded using an EPC-9 patch-clamp amplifier (HEKA Electronics, Lambrecht/Pfalz, Germany). The beta cells were identified by the lack of inward Na^+ currents in the presence of a depolarising pulse from −70 to 0 mV (5 ms in duration) [18]. The capacitance measurements were performed using software-based lock-in software (Pulse version 8.11; HEKA Electronics). The changes in cell capacitance were estimated by the Lindau–Neher technique [19, 20] by implementing the 'Sine + DC' feature of the lock-in module. The amplitude of the sine wave was 20 mV and the frequency was set at 1250 Hz. Patch pipettes (tip resistance 5–7 MΩ when filled with the pipette solution) were pulled from borosilicate tubing. The capacitance measurements were performed at 32–34°C. Capacitance was measured again 2 min 30 s after treatment with or without adiponectin. The standard extracellular medium consisted of 120 mmol/l NaCl, 20 mmol/l tetraethylammonium-Cl, 3.6 mmol/l KCl, 2 mmol/l $NaHCO_3$, 0.5 mmol/l NaH_2PO_4, 0.5 mmol/l $MgSO_4$, 5 mmol/l HEPES (at pH 7.4), 2.6 mmol/l $CaCl_2$ and 5 mmol/l D-glucose. The pipette solution for the perforated patch was composed of 76 mmol/l Cs_2SO_4, 10 mmol/l NaCl, 10 mmol/l KCl, 1 mmol/l $MgCl_2$ and 5 mmol/l HEPES (at pH 7.35).

The cytosolic Ca^{2+} concentration ($[Ca^{2+}]_c$) was measured using fura-2 by exciting its fluorescence in a dual-wavelength ratiometric mode at 340 and 380 nm. The emission wavelength was filtered at 500 nm. $[Ca^{2+}]_c$ was expressed as the 340:380 nm ratio.

Western blot analysis Mouse islets were homogenised in ice-cold buffer A (25 mmol/l Tris-HCl; pH 7.4, 10 mmol/l sodium orthovanadate, 10 mmol/l sodium pyrophosphate, 100 mmol/l sodium fluoride, 10 mmol/l EDTA, 10 mmol/l EGTA and 1 mmol/l phenylmethylsulfonyl fluoride). Samples were separated on polyacrylamide gels and transferred to a nitrocellulose membrane (Schleicher & Schuell, Dassel, Germany). Rabbit anti-phospho-AMPKα (Thr-172) antibody and rabbit AMPKα antibody were purchased from Cell Signaling (Beverly, MA, USA).

Total internal reflection fluorescence microscopy We performed total internal reflection fluorescence (TIRF) microscopy using an inverted microscope (IX70; Olympus, Tokyo, Japan) with a high-aperture objective lens (Apo 100× OHR, Na 1.65; Olympus) as described previously [21, 22]. Mouse pancreatic islets were isolated by collagenase digestion. Isolated islets were dissociated into single cells by incubation in Ca^{2+}-free KRB containing 1 mmol/l EGTA and the beta cells were cultured on high-refractive-index glass (Olympus) coated with fibronectin (Koken, Tokyo, Japan). To label the insulin-containing granules, pancreatic beta cells were infected with recombinant adenovirus Adex1CA insulin green fluorescent protein (GFP) as described previously [22]. The experiments were performed 2 days after infection. To observe GFP, we used a 488 nm laser line for excitation. The procedure used to monitor the motion of GFP-labelled insulin granules in pancreatic beta cells by TIRF microscopy has been described elsewhere [21]. Infected cells on a glass coverslip (Olympus) were mounted in an open chamber and incubated for 30 min at 37°C in KRB and 0.3% (wt/vol.) bovine serum albumin in the presence of 2.8 mmol/l glucose. The cells were then transferred to a thermostatically controlled stage (37°C) and stimulated with 10 μg/ml adiponectin in the presence of 5.6 mmol/l glucose in the chamber. Diodomethane sulphur immersion oil (Cargille Laboratories, Cedar Grove, NJ, USA) was used to establish contact between the objective lens and the coverslip. The space constant for the exponential decay of the evanescent field was approximately 43 nm.

Image acquisition and analysis Images were acquired every 300 ms with a cooled charge-coupled-device camera (DV887DCSBV; Andor Technology, South Windsor, CT, USA) operated with Metamorph 6.2 software (Universal Imaging, Downingtown, PA, USA). Most analyses, including tracking (single projection of difference images) and area calculations, were performed with the Metamorph software. To analyse the data, fusion events were selected

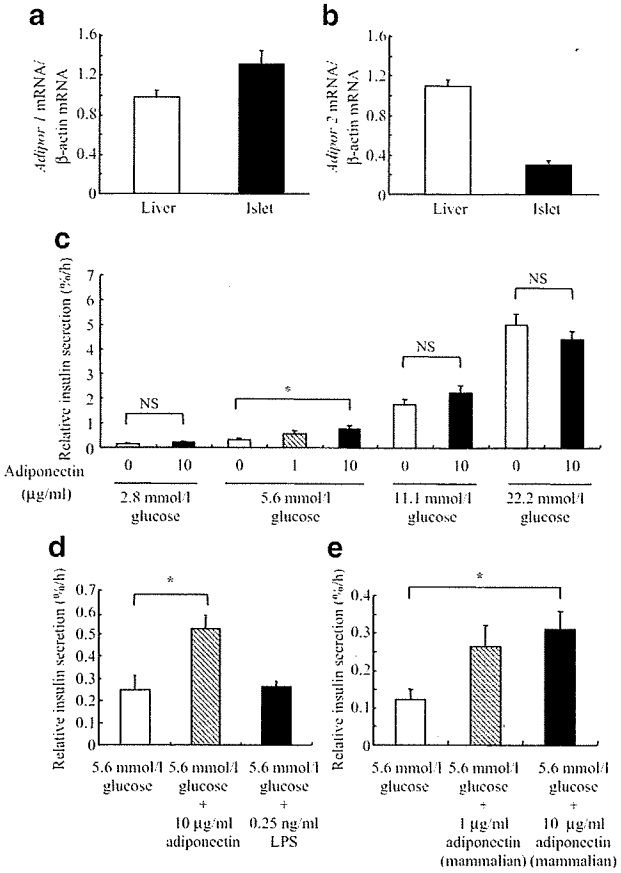

Fig. 1 Adiponectin stimulates insulin secretion from islets. TaqMan RT-PCR of *Adipor1* (n=3) (**a**) and *Adipor2* (n=3) (**b**) in mouse pancreatic islets. **c** Islets were incubated in KRB containing the indicated concentrations of glucose with or without adiponectin (n=9–20). **d** Islets were incubated with glucose and with adiponectin or LPS (n=3). **e** Islets were incubated with glucose with or without mammalian-derived adiponectin (n=3). Values are means±SEM. *p<0.05

manually and the average fluorescence intensity of the individual granules in a 1×1 μm square placed over the granule centre was calculated. The number of fusion events was counted manually while looping approximately 15,000 time-lapsed frames. The sequences were exported as single TIRF files and further processed using Adobe Photoshop 6.0 software or converted into Quick Time movies.

Insulin secretion study in vivo Four days before the insulin secretion study, a catheter consisting of a silicone part (Phicon Tube; Fuji Systems, Tokyo, Japan) and a polyethylene part (PE-50; BD Biosciences, Franklin Lakes, NJ, USA) was inserted into the right jugular vein of animals under general anaesthesia with sodium pentobarbital, to administer infusions. The studies were performed on the mice under conscious, unstressed conditions after 24 h fast. D-Glucose (0.2 g/kg) was injected intravenously through the catheter, either alone or with 0.6 mg/kg adiponectin. Blood samples were collected into a heparinised tube before and 10 and 20 min after the injection. After immediate centrifugation, the plasma was separated and stored at −20 °C until analysed.

Insulin levels were determined by radioimmunoassay. The insulin to glucose ratio was calculated using the formulas: (10 min insulin level−fasting insulin level)/(10 min blood glucose level−fasting blood glucose) or (20 min insulin level−fasting insulin level)/(20 min blood glucose level−fasting blood glucose level). The adiponectin levels were determined with a mouse adiponectin ELISA kit (Otsuka, Tokyo, Japan). All data were obtained from six independent experiments.

Statistical analysis The statistical significance of differences between groups was determined using Student's t test for unpaired comparisons, the Welch test, Dunnett's t test or Steel's z test. A p value of <0.05 was regarded as significant.

Results

Adiponectin stimulates insulin secretion from mouse pancreatic islets at low glucose concentration We first confirmed the expression of *Adipor1* and *Adipor2* in mouse pancreatic islets (Fig. 1a,b), obtaining results that were essentially consistent with those previously reported [12]. We next examined the effect of adiponectin on glucose-induced insulin secretion from isolated islets during a 60 min static incubation (Fig. 1c). Adiponectin significantly stimulated insulin secretion to 2.3-fold the baseline value at a 5.6 mmol/l glucose concentration (p=0.012; Fig. 1c). However, adiponectin did not significantly increase insulin secretion in the presence of 11.1 or 22.2 mmol/l glucose. Since high concentrations of lipopolysaccharide (LPS) have been reported to stimulate insulin secretion from islets [23], we investigated the effect of LPS on insulin secretion from islets at 5.6 mmol/l glucose. When mouse pancreatic islets were treated with LPS at the same quantity as was present in recombinant adiponectin derived from *Escherichia coli*, no effect of LPS was found on insulin secretion (Fig. 1d). In addition, 10 μg/ml mammalian-derived adiponectin also stimulated insulin secretion from mouse pancreatic islets (p=0.039; Fig. 1e). These results suggest that adiponectin acts directly on beta cells to increase insulin secretion.

Adiponectin stimulates insulin secretion without causing ATP generation, palmitic acid oxidation or cAMP generation in islets To examine the effect of adiponectin on ATP generation, we measured glucose-induced changes in D-[6-^{14}C] glucose oxidation and the ATP content of islets (Table 1). D-[6-^{14}C]Glucose oxidation to $^{14}CO_2$ in the control islets increased 5.5-fold when the extracellular glucose concentration was raised from 5.6 to 22.2 mmol/l. Adiponectin at a concentration of 10 μg/ml did not affect D-[6-^{14}C]glucose oxidation in the presence of 5.6 mmol/l of glucose

compared with control. In the presence of 22.2 mmol/l glucose, adiponectin also failed to significantly change D-[6–^{14}C]glucose oxidation compared with control islets incubated at the same glucose concentration. Next, we measured the ATP content of islets to directly monitor the efficiency of mitochondrial ATP synthesis. The results showed that adiponectin at a concentration of 10 μg/ml did not affect ATP content in the presence of 5.6 mmol/l glucose (Table 1). The above findings indicate that adiponectin has no stimulatory effect on ATP generation from mitochondrial glucose metabolism. Increase in cAMP content potentiates glucose-stimulated insulin secretion through activation of cAMP-dependent protein kinase [24]. Adiponectin also failed to significantly change the cAMP content as compared with control islets (Table 1). Although adiponectin has been reported to reduce elevated fatty acid levels in muscle by oxidising fatty acids [7–9], no significant change in the oxidation of palmitic acid was observed in pancreas islets treated with adiponectin as compared with control at 5.6 or 22.2 mmol/l of glucose (Table 1).

Adiponectin stimulates insulin secretion without causing membrane depolarisation, closure of K^+_{ATP} – channels or Ca^{2+} entry into the cytosol We measured the membrane potentials of pancreatic beta cells to determine whether adiponectin caused membrane depolarisation. In the presence of 5.6 mmol/l glucose, adiponectin at a concentration of 10 μg/ml had no effect on the membrane potentials (Fig. 2a), but membrane of pancreatic beta cells depolarised when the extracellular glucose level was raised from 5.6 to 22.2 mmol/l (Fig. 2a). Figure 2b shows the current–voltage relationship for Ca^{2+} currents. When the membrane potential was held at −70 mV, Ca^{2+} currents elicited by 200 ms depolarising voltage-clamp pulses from −40 to 40 mV were applied in the presence of 5.6 mmol/l glucose. Adiponectin at a concentration of 10 μg/ml did not change the current–voltage curve via Ca^{2+} influx into the cytosol (Fig. 2b). To investigate the effect of adiponectin on the increase in the $[Ca^{2+}]_c$, we monitored the fluorescence of fura-2/acetoxymethyl ester excited at 340 and 380 nm in perifused islets (Fig. 2c). The 340:380 nm fluorescence ratio increased in islets when the glucose concentration was raised from 5.6 to 22.2 mmol/l, but adiponectin had no effect on the $[Ca^{2+}]_c$ (Fig. 2c). To clarify whether adiponectin stimulates insulin secretion without causing Ca^{2+} influx, we next investigated the effects of adiponectin on mouse pancreatic islets in the presence of the L-type Ca^{2+}-channel blocker, nitrendipine. Nitrendipine at a concentration of 5 μmol/l is known to inhibit Ca^{2+} influx [25]. Nevertheless, insulin secretion was markedly diminished at 22.2 mmol/l glucose in the presence of nitrendipine, whereas adiponectin significantly stimulated insulin secretion at 5.6 mmol/l glucose (p=0.043; Fig. 2d). Interestingly, adiponectin also significantly stimulated insulin secretion at 22.2 mmol/l glucose concentration in the presence of nitrendipine (p=0.047) (Fig. 2d). These findings suggest that adiponectin is able to stimulate insulin secretion when the influx of Ca^{2+} through voltage-dependent Ca^{2+} channels is blocked.

AMPK is not involved in adiponectin-stimulated insulin secretion Adiponectin has been previously reported to improve insulin sensitivity in muscle and liver by enhancing fatty acid oxidation via the activation of AMPK [7, 8], which has been found to increase glucose transport by stimulating the translocation of GLUT4 [26, 27]. To elucidate whether AMPK might be involved in adiponectin-stimulated insulin secretion, we examined the effect of adiponectin on phosphorylation of AMPK in mouse pancreatic islets. However, adiponectin did not affect the phosphorylation of AMPK at 5.6 mmol/l glucose (Fig. 3a). The AMPK activator 5-amino-imidazole-4-carboxamide riboside (AICAR), on the other hand, significantly increased the phosphorylation of AMPK at 5.6 mmol/l glucose (p=0.00083; Fig. 3b). However, AICAR significantly decreased insulin secretion from mouse pancreatic islets (p=0.024; Fig. 3c) [28]. These results suggest that AMPK is not involved in adiponectin-stimulated insulin secretion at low glucose concentrations.

Adiponectin stimulates insulin release via induction of increased fusion events at a low glucose concentration We

Table 1 Adiponectin stimulates insulin secretion without causing ATP generation, palmitic acid oxidation or cAMP generation in islets

	D-[6–^{14}C]Glucose oxidation (pmol h^{-1} islet^{-1})		ATP content (pmol/islet)	[U-^{14}C]Palmitic acid oxidation (fmol h^{-1} islet^{-1})		cAMP content (fmol/islet)
Glucose (mmol/l)	5.6	22.2	5.6	5.6	22.2	5.6
Control	1.92±0.27	10.6±1.1[b]	1.16±0.09	2.98±0.20	2.41±0.07[a]	49±7
n	4	4	5	4	4	5
Adiponectin	2.37±0.22	11.7±1.8[b]	1.29±0.08	3.23±0.23	2.59±0.10[a]	62±10
n	4	4	5	4	4	5

Values are means±SEM.
[a]p<0.05, [b]p<0.01 compared with the 5.6 mmol/l glucose group